



저작자표시-비영리-변경금지 2.0 대한민국

이용자는 아래의 조건을 따르는 경우에 한하여 자유롭게

- 이 저작물을 복제, 배포, 전송, 전시, 공연 및 방송할 수 있습니다.

다음과 같은 조건을 따라야 합니다:



저작자표시. 귀하는 원저작자를 표시하여야 합니다.



비영리. 귀하는 이 저작물을 영리 목적으로 이용할 수 없습니다.



변경금지. 귀하는 이 저작물을 개작, 변형 또는 가공할 수 없습니다.

- 귀하는, 이 저작물의 재이용이나 배포의 경우, 이 저작물에 적용된 이용허락조건을 명확하게 나타내어야 합니다.
- 저작권자로부터 별도의 허가를 받으면 이러한 조건들은 적용되지 않습니다.

저작권법에 따른 이용자의 권리는 위의 내용에 의하여 영향을 받지 않습니다.

이것은 [이용허락규약\(Legal Code\)](#)을 이해하기 쉽게 요약한 것입니다.

[Disclaimer](#)

A MASTER'S THESIS

**Exploration of senescence-regulatory  
genes for extension of the greening  
period in *Zoysia japonica* through  
transcriptome analysis of leaf  
senescence**

WANG LANSHUO

(Supervised by professor Jeongsik Kim)

Department of Interdisciplinary Graduate Program in  
Advanced Convergence Technology and Science

GRADUATE SCHOOL

JEJU NATIONAL UNIVERSITY

December 2022

**Exploration of senescence-regulatory genes for  
extension of the greening period in *Zoysia japonica*  
through transcriptome analysis of leaf senescence**


**WANG LANSHUO**

(Supervised by professor Jeongsik Kim)



A thesis submitted in partial fulfillment of the requirement for the degree of  
Master of Interdisciplinary Graduate Program in Advanced Convergence  
Technology and Science

2022. 12. 09

This thesis has been examined and approved.

Jin Hee Kim 

Thesis director, Dr. Jin Hee Kim, Research Prof. of Subtropical Horticulture  
Research Institute, Jeju National University

Hong-Gyu KANG   
Jeongsik KIM 

(Name and signature)

\_\_\_\_\_ Date

**Department of Interdisciplinary Graduate Program in Advanced  
Convergence Technology and Science  
GRADUATE SCHOOL  
JEJU NATIONAL UNIVERSITY**

## Contents

|  |           |
|--|-----------|
| <b>LIST OF FIGURES</b> .....   | <b>I</b>  |
| <b>LIST OF TABLES</b> .....  | <b>II</b> |
| INTRODUCTION .....   | 1         |
| MATERIAL AND METHODS.....  | 6         |
| Plant material and growth conditions .....   | 6         |
| Plasmid constructions .....  | 6         |
| Assay for dark-, salt-, and age-induced senescence.....  | 7         |
| RNA sequencing and bioinformatic analysis .....  | 8         |
| Gene expression analysis by qRT-PCR.....   | 9         |
| Transient expression in Arabidopsis protoplasts .....  | 10        |
| Transient expression mediated by <i>Agrobacterium</i> in <i>Nicotiana benthamiana</i><br>.....   | 11        |
| RESULTS .....  | 15        |
| Preparation of leaf samples for comparative transcriptome analysis of age-,<br>dark- and salt-induced senescence in <i>Z. japonica</i> ..... | 15        |
| Transcriptomic comparison of age, dark, and salt-induced senescence .....  | 20        |
| Functional characterization of transcriptomic responses in age-, dark-, and<br>salt-induced senescence .....                                 | 25        |
| Identification of differentially expressed genes.....  | 28        |
| Validation of qRT-PCR of differentially expressed genes in each senescence<br>condition .....  | 31        |

|   |    |
|---|----|
| Identification and expression profile of TF cDEGs.....  | 35 |
| Effect of TF candidate genes in the <i>Z. japonica</i> senescence promoters in a<br>protoplast-mediated transient expression system ..... | 43 |
| Functional assessment of TF candidate genes for the regulation of senescence<br>responses in heterologous tobacco leaves.....             | 46 |
| DISCUSSION.....   | 48 |
| CONCLUSION.....   | 53 |
| REFERENCES .....  | 55 |
| ACKNOWLEDGMENT .....  | 62 |

## LIST OF FIGURES

|   |    |
|---|----|
| <b>Figure 1.</b> Preparation of leaf samples for comparative transcriptome analysis of age-, dark- and salt-induced senescence in <i>Z. japonica</i> .....                    | 18 |
| <b>Figure 2.</b> PCA analysis for transcriptome responses in <i>Z. japonica</i> leaves under the different senescence conditions .....  | 24 |
| <b>Figure 3.</b> Gene set enrichment analysis for transcriptome profiles in each senescence condition .....   | 27 |
| <b>Figure 4.</b> Comparison of the number of differentially expressed genes in different senescence-induced conditions .....  | 30 |
| <b>Figure 5.</b> Specifically responsive genes in each senescence condition .....   | 32 |
| <b>Figure 6.</b> qRT-PCR-based validation of DEGs that were responsive in each senescence condition through RNA-seq analysis .....  | 34 |
| <b>Figure 7.</b> Expression of <i>Z. japonica</i> TFs in response to all senescence conditions.....<br>.....  | 37 |
| <b>Figure 8.</b> qRT-PCR-based validation of TF DEGs that were responsive in all senescence condition examined through RNA-seq analysis .....                                 | 39 |
| <b>Figure 9.</b> Kinetic expression pattern of TF DEGs identified by RNA-seq analysis along senescence.....   | 41 |
| <b>Figure 10.</b> Functional analysis of putative TF candidate genes through effector and reporter assay in <i>Arabidopsis</i> protoplasts .....                              | 45 |
| <b>Figure 11.</b> Dark-induced senescence responses when TF candidate genes were over-expressed in tobacco using an <i>Agrobacterium</i> -mediated transient expression ..... | 47 |

## LIST OF TABLES

|   |    |
|---|----|
| <b>Table 1.</b> List of gene-specific PCR primer sequences for cloning..... | 13 |
| <b>Table 2.</b> List of PCR primers of genes that used for qRT-PCR.....     | 14 |
| <b>Table 3.</b> Raw Data Statistics .....                                   | 22 |
| <b>Table 4.</b> Mapping status of 15 samples .....                          | 23 |

## INTRODUCTION

The genus *Zoysia* Willd. is a member of the tribe Zoysieae, which is part of the subfamily Chloridoideae. *Zoysia* species are widespread in temperate Northeast Asia, including Korea and Japan, as well as tropical China and Southeast Asia. *Zoysia japonica*, commonly known as zoysiagrass, Korean lawngrass, or Japanese lawngrass, is a popular warm-season C4 turf species with numerous advantageous traits such as low care and great resistance to environmental challenges such as heat, drought, and traffic (Teng et al., 2016b). However, the shorter green phase of *Z. japonica* relative to other cool-season turfgrasses has become a significant impediment to its widespread use. For a long time, turf breeders have put lots of effort to develop *Z. japonica* species with a longer and healthier green period (Loch et al., 2016; Teng et al., 2016b).

Leaf senescence occurs in their final stage of growth and is evolutionally acquired processes as energy reutilization strategies in plants (Mahmood et al., 2022). Leaves are photosynthetic organs that produce chemical energy and building units for macromolecules and accumulate cellular materials in growth periods. During leaf senescence, chloroplasts begin to degrade and their macromolecules, which include lipids, proteins, and nucleic acids, are disassembled and transferred to growing organs such as new shoots, young leaves, seeds, or flowers. (Guo et al., 2021). Premature and delayed senescence can affect the quality and yield of offspring in plants by reduction in accumulation and remobilization periods, respectively, and appropriate onset of senescence is crucial for maximizing succession of their progenies. These imply that leaf senescence is adopted as a life history strategy with significant biological



consequences. Onset of leaf senescence is determined by the coordinated actions among senescence regulatory genes that are regulated tightly at various levels, including chromatin, mRNA (by transcriptional and post-transcriptional regulation) and protein (by translational and post-translational regulation) levels. During leaf senescence, expression of thousands of senescence-associated genes (SAGs) involved across many molecular and physiological processes are regulated at the transcriptional level (Kim et al., 2014). The identification of the multiple transcription factors (TFs) that are involved in the leaf senescence regulation has demonstrated the significance of TF-mediated transcriptional control. Several TF families, including MYC, NAC, bHLH, and WRKY, are commonly involved in the regulation of leaf senescence in a wide range of plants. Regulatory WRKY genes in leaf senescence include WRKY75, WRKY53, WRKY70, WRKY22, WRKY54, and WRKY6, which acts collaboratively and independently (Robatzek and Somssich, 2001; Miao et al., 2004; Zhou et al., 2011; Besseau et al., 2012; Zhang et al., 2021a). For example, WRKY54 and WRKY70 interact and cooperatively represses leaf senescence, which are independently with WRKY30 (Besseau et al., 2012). WRKY53 and WRKY30 are involved in senescence through reactive oxygen signals, separated from WRKY54 and WRKY70. The NAC TF family, one of the plant biggest gene families is also essential for controlling leaf senescence. In *Arabidopsis*, more than half of the NAC family genes undergo altered expression during leaf senescence (Kim et al., 2016a). Comprehensive and intensive investigation of functional roles of NACs performed by many different research groups revealed that many NACs have been discovered as positive (*ORE1*, *ANAC016*, *ORS1*, and *AtNAP*) or negative (*JUB1* and *VNI2*) regulators during leaf senescence

(Podzimska-Sroka et al., 2015). To coordinate expression of downstream genes during leaf senescence, members of the WRKY and NAC families interact and co-work to regulate onset of leaf senescence by either activating or inhibiting transcription or by forming protein complexes (Zentgraf et al., 2010; Besseau et al., 2012; Kim et al., 2016a; Kim et al., 2018a). The basic helix-loop-helix (bHLH) transcription factors effectors also control leaf senescence. MYC2, MYC3, and MYC4 are the subgroup IIIe bHLH TFs that have redundant activities and stimulate JA-induced leaf senescence, with MYC2 attaching to and activation the promoter of the *SAG29* gene (Qi et al., 2015). On the other hand, The bHLH17, bHLH03, bHLH14, and bHLH13, subgroup IIIId of bHLH factors connect to the promoter of *SAG29* and suppress the expression of MYC2-activated *SAG29* to prevent JA-induced leaf senescence (Qi et al., 2015). Furthermore, there is mounting evidence that MYBs are implicated in leaf senescence. In addition to regulating the transcription of downstream SAGs, these senescence-related TF regulatory networks respond to a multitude of internal and external senescence-triggering signals, including as hormones, aging, darkness, salinity, heat, and disease (Buchanan-Wollaston et al., 2005; Lim et al., 2007a; Park et al., 2007; Breeze et al., 2011; Allu et al., 2014). Since senescence can be induced by a variety of internal developmental and external environmental cues, the transcriptional regulation of SAGs under different senescence-inducing conditions needs to be investigated to decipher common and unique aspects of their transcriptional regulation (Zhang et al., 2014). The comparative transcriptomic approaches can allow us to select potential senescence regulatory genes which can delay the onset of senescence conferring a prolonged green period of *Z. japonica*.

Next generation sequencing (NGS)-based RNA sequencing (RNA-seq) enable the identification of transcripts and the prospective finding of genes implicated in diverse biological processes. Our understanding of the interactions between plants and the environment has significantly improved in recent years as a result of the development of RNA-seq as a potent method for the discovery and identification of genes implicated in abiotic stressors (Cheng et al., 2009). In addition, continuous refinement and routine annotation updates are required for correctly interpreting the functional elements of the genome. *P. japonica* genome sequence resources were published in 2016 (Tanaka et al., 2016), but their gene annotations are at the primitive stage and no subsequent updates have been made in the National Center for Biotechnology Information (NCBI) database. Generation of *Z. japonica* genetic resources is constrained by a lack of complete genome annotation. Temporal and spatial RNAs-seq analysis during senescence can improve accuracy of genome structure in *Z. japonica*.

Over the last 30 years, significant advances have been made in our comprehension of the fundamental molecular mechanisms governing leaf senescence in Arabidopsis (Kim et al., 2018b). Practical value of senescence programs in applications also accelerates the molecular and genetic studies on leaf senescence in agricultural crops (Guo and Gan, 2014) including rice (Lee et al., 2001; Lee and Masclaux-Daubresse, 2021), and tobacco (Uzelac et al., 2016), wheat (Uauy et al., 2006), maize (Zhang et al., 2014), and cotton (Kong et al., 2013). However, a few studies on *Z. japonica* leaf senescence have been reported, although senescence in turfgrasses is of particular interest due to potential increase in their economic values by affecting senescence-related phenotypes including visual greenness, nutritional level, and biomass

accumulation (Teng et al., 2016b). Mutation in *ZjSGR*, *ZjPPH*, and *ZjNOL* that are involved in chlorophyll degradation induced stay-green phenotypes (Teng et al., 2016a; Teng et al., 2021; Guan et al., 2022). Additionally, around 200 SAGs were isolated as potential senescence markers based on subtractive hybridization from dark induced leaf senescence in zoysiagrass (Cheng et al., 2009). To date, available genetic resources for senescence study in zoysiagrass are largely limited (Wei et al., 2015; Tanaka et al., 2016), and its senescence mechanisms are far from fully elucidated.

In this study, I performed a comparative RNA-seq analysis in age-, dark- and salt-induced leaf senescence for elucidation of the molecular basis of *Z. japonica* senescence and identification of key senescence regulatory genes. Differentially expressed genes (DEGs) were identified in each senescence condition and a group of DEGs responding specifically to each senescence has been validated as specific molecular markers for each senescence condition. Functional categorization of DEGs suggested unique and common biological processes associated with senescence conditions. In addition, seven TF genes responsive to all senescence conditions have been identified as potential senescence regulatory genes through a protoplast-mediated transient expression system. This study provides a molecular basis for understanding *Z. japonica* leaf senescence and gene resources for genetic modification to extend the leaf greening period in *Z. japonica*.

## MATERIAL AND METHODS

### Plant material and growth conditions

Zoysiagrass used in all experiments was *Zoysia japonica* Steud cv Duckchang (wide-leaf variety; Duckchang Agri-Business Co., Korea). In a greenhouse (only supplemented with white LED light (4000K neutral white) at cloudy or rainy days; at 30~35 °C at day and 20~25°C at night), *Z. japonica* plants were planted and grown on soil. For senescence assay, underground runners were transferred into new soil, and 4<sup>th</sup> leaves that emerged from sprouts were cut into 3 pieces of which middle parts were used for all assays. Leaf age was counted as days after leaf emergence (DAE).

### Plasmid constructions

Pfu-X DNA polymerase (Solgent, Korea) was used to amplify candidate transcription factors (TFs) or promoters using the appropriate primer sets (Table 1) and *Z. japonica* leaf cDNA and genomic DNA as a template, respectively. The PCR products were subcloned into the PCR-CCD-F entry vector after being digested with the appropriate restriction enzymes. GATEWAY cloning technology (Invitrogen, USA) was applied to generate plasmid constructs for the effector and reporter in the protoplast-mediated transient expression assay. For overexpression effectors in protoplasts, the gateway version of pCsVMV-eGFP-N-999 was used for recombination with corresponding entry clones to generate effector plasmids of ZjNAP-, ZjWRKY75-, ZjNAC1-, ZjAZF2-, ZjNAC083-, ZjARF1-, ZjPIL5-, and ZjHB2-pCsVMV-eGFP-N-999 (Kim and Somers, 2010). For tobacco transient expression, the gateway variant of pCsVMV-

eGFP-N-1300 was used for recombination with the suitable entrance clones to generate the effector plasmids of pCsVMV-ZjNAP-eGFP-N-1300 and pCsVMV-ZjNAC1-eGFP-N-1300. For reporter plasmids in protoplast including ZjSGR- and ZjPCAP-LUC, promoter-LUC final constructs were built by LR recombination using the corresponding entry clone and the gateway version of the gateway version of pOmegaLUC\_SK<sup>+</sup>-GW vector.

### **Assay for dark-, salt-, and age-induced senescence**

The middle parts of leaves at DAE21 were used for dark or salt-induced senescence assay or as a mature green sample (Hayakawa et al., 2006) for the control in age-induced senescence. In the dark-induced leaf senescence experiment, fragments of leaves were floating upside down on 3 mM MES buffer (pH 5.7) in 12-well plates completely enclosed in aluminum foil. Leaf samples were incubated at 25 °C for the indicated days and were collected at 4–5 hours after light-on. For salt-induced leaf senescence, leaf samples were prepared as described for dark assay, except for their incubation in 3 mM MES buffer, supplemented with 150 or 180 mM salt under 16 h light/ 8 h dark conditions. For age-induced senescence, the middle region of the 4th leaves, at the indicated age and DAE 49 for RNA-seq analysis, was collected at 4–5 h after light-on. The collected leaf samples were either used to quantify the amount of chlorophyll and photochemical efficiency or kept at -80 °C for further gene expression or transcriptome analysis. Eight to twelve leaves per an assay were used to determine the amount of chlorophyll using a CCM-300 (Opti-Sciences, USA) and the photochemical efficiency using a Pocket PEA fluorimeter (Hansatech Instruments,

England). At least nine leaves were collected in each condition for gene expression or transcriptome analysis, and three biologically independent samples were prepared by transferring independent underground runners.

### **RNA sequencing and bioinformatic analysis**

Total RNA was extracted from all collected samples using Welprep (South Korea). Total RNA integrity was determined using the RNA Pico 6000 chip kits of the Agilent Technologies 2100 Bioanalyzer (RNA integrity No. >7.0). The RNA-seq was performed at the Macrogen company (South Korea). The TruSeq Stranded mRNA LT Sample Prep Kit for Illumina platform was used to create the mRNA-seq libraries in accordance with the manufacturer's instructions. Three independent sample sets were used as biological replicates, and the generated library was subjected to pair-end 101-nt sequencing on a Novaseq 6000 system. The quality of raw sequences and trimmed sequences were checked by FastQC ver 0.11.7. Raw sequence reads were preprocessed by removing adaptor sequences and trimming low-quality ends using the Trimmomatic v0.38 program (Bolger et al., 2014). The preprocessed reads were aligned to the *Zoysia japonica* ssp. *nagirizaki* genome draft (Tanaka et al., 2016) using the HISAT2 software (v2.1.0) with a default setting (Kim et al., 2019). The reads in the annotated genes were assembled using StringTie v2.1.3b (Pertea et al., 2015) based on the new *Zoysia* genome annotation files we created, the abundance of gene expression was calculated in the reads, and the expression was normalized to fragments per kilobase million (FPKM) values for each sample. Genes with more than one count were used for statistical analysis for each pair-wise comparison.

The differential expressed genes (DEGs) in each senescence-induced condition was selected using the DESeq2 on GALAXY, based on regularized log (rlog) transformed values of FPKM and Relative Log Expression (RLE) normalization (Love et al., 2014). The selection criteria of DEGs were the log<sub>2</sub> fold-change (FC) cut-off of > 1 and an adjusted p-value cut-off of < 0.05 by applying the nbinomWaldTest function. Functional analysis of all DEGs was performed using MapMan (Thimm et al., 2004) and the data were visualized using PageMan (Usadel et al., 2009). A critical value of 0.05 (equivalent to a |Z-core| ≥ 1.96) was used to select enriched functional categories.

### **Gene expression analysis by qRT-PCR**

Frozen leaf tissues were ground using a Retsch mix mill MM400 and used for RNA extraction. Total RNA was extracted from ground tissues using WelPrep (South Korea) and processed with DNase I (Ambion, USA). DNA-free RNA was reverse-transcribed in a 10-μL reaction using an oligo (dT15) primer and ImProm-II<sup>TM</sup> reverse transcriptase (Promega, USA). Following a 12-fold dilution, 3 μL of diluted cDNA was amplified by real-time PCR using TOPreal<sup>TM</sup> qPCR 2X PreMIX (Enzynomics, Korea) and CFX96 real-time qPCR detection system (Bio-Rad, USA). The gene-specific primers given in the primer lists (Table 2) were used to quantitative the relevant transcript levels. A 15 μL reaction volume containing 7.5 μL SYBR mixture, 3 μL cDNA, 1.5 μL gene-specific primers, and 3 μL ddH<sub>2</sub>O was used for qRT-PCR. The PCR program parameters were 95°C for 10 minutes, followed by 40 cycles of 95°C for 10 sec, 60°C for 15 sec, 72°C for 30 sec, and a melting curve stage of 65°C



for 5 sec and 95°C for 1 min. The comparative CT approach was used to quantify fold changes in gene expression (Livak and Schmittgen, 2001), with *ZjACT* serving as the reference gene. Relative gene expression in kinetic analysis were calculated by the ratio of gene expression level in each condition to the maximal levels in wild-type samples. Two biological trials were carried out at least.

### **Transient expression in Arabidopsis protoplasts**

Protoplast isolation and DNA transfections were performed as described previously (Doan et al., 2022). 15 to 25 leaves of 3- to 4-week-old Col-0 plants were treated for 30 seconds with 70% ethanol and followed by being rinsed twice using sterile water. After being scratched with sandpaper lightly, the leaves were incubated for 2.5 hours at room temperature in 10 mL of cell wall digestion enzyme solution (1% Cellulase R10, 0.5% Macerozyme R10 (Yakult Honsha, Japan), 400 mM mannitol, 20 mM KCl, 10 mM CaCl<sub>2</sub>, 20 mM MES-KOH (pH 5.7), and 0.1% BSA (Sigma A6793, United States)). The protoplast solutions were filtered with 100 μm nylon mesh and centrifuged at 100 g for 5 minutes in a round-bottom culture tube. The supernatant protoplasts were washed with 1 mL of W5 solution (154 mM NaCl, 125 mM CaCl<sub>2</sub>, 5 mM KCl, 1.5 mM MES-KOH [pH 5.7], and 5 mM Glucose) and placed on ice for 30 min. The protoplasts were harvested and resuspended in MMG solution (400 mM mannitol, 15 mM MgCl<sub>2</sub>, and 4 mM MES-KOH [pH 5.7]), with a final cell concentration of  $2 \times 10^5 \text{ mL}^{-1}$ . In addition, plasmid mixtures containing 20 μl effector, 5 μl reporter, and 0.2 μl internal control (35S-RLUC) were added into 200 μl of protoplasts in MMG solution. Plasmid DNAs used for transfection was prepared by

using a CsCl gradient ultracentrifugation. Protoplasts containing plasmid DNAs were transfected by adding 230  $\mu\text{l}$  (1 vol.) of polyethylene glycol (PEG) solution [40% PEG-4000, 200 mM mannitol, and 100 mM  $\text{Ca}(\text{NO}_3)_2$ ] and further incubated for 8 to 15 minutes at room temperature. The protoplast-DNA-PEG combination was diluted with 920  $\mu\text{l}$  (2 vol.) of W5 solution. After 1 min centrifugation at 100 x g, protoplasts transfected were resuspended in 700  $\mu\text{l}$  of W5 solution containing 5% fetal bovine serum (Sigma F4135, United States) and 50  $\mu\text{g ml}^{-1}$  ampicillin. A total of 300  $\mu\text{l}$  of transfected protoplasts were placed into each well of a white 96-well microplate containing 3  $\mu\text{l}$  of LUC substrate (5 mM luciferin, Goldbio LUCK-250, Netherlands) or 3  $\mu\text{l}$  of RLUC substrate (10  $\mu\text{M}$  Coelenterazine-native, Sigma C2230, United States). The microplate was sealed with a transparent plastic cap and incubated on a GloMax 96 microplate luminometer (Promega, United States) at 22°C in the dark condition. Luminescence levels were measured every 30 min for three days. Relative LUC reporter activity was measured by normalization of each data set's firefly luciferase bioluminescent level to the highest RLUC level for the entire measurement.

#### **Transient expression mediated by *Agrobacterium* in *Nicotiana benthamiana***

*Agrobacterium* carrying indicated plasmids that were cultured overnight was collected and resuspended in resuspension solution (10 mM MES, 10 mM  $\text{MgCl}_2$ , and 100  $\mu\text{M}$  acetosyringone). *Nicotiana benthamiana* plants were cultivated in a climate chamber (16-h light/ 8-h dark photoperiod, 22°C). *Agrobacteria* cells with effector plasmid were mixed with the *Agrobacteria* with P19 silencing suppressor in the right ratio, and mixed *Agrobacteria* solution were injected with a 1-ml needleless syringe into 6-week-

old *N. benthamiana* leaves. Agrobacterium carrying an empty GFP vector used as a control. Tobacco leaves were detached at 1 day after infiltration and incubated in the dark for 7 d. Chlorophyll levels and photochemical efficiency were measured using CCM-300 (Opti-Sciences, USA) and a Pocket PEA fluorimeter (Hansatech Instruments, England), respectively.

**Table 1. List of gene-specific PCR primer sequences for cloning**

| Primer Name       | Sequence (5' to 3')                       | R.E.*          |
|-------------------|---|----------------|
| <i>ZjNAP-F</i>    | TTT <u>ACTAGT</u> ATGGCGACGAGGATGCCTT     | <i>SpeI</i>    |
| <i>ZjNAP-R</i>    | TTT <u>AAGCTT</u> CTGGTTCAGGAACGGGTGGCTA  | <i>HindIII</i> |
| <i>ZjWRKY75-F</i> | TTT <u>CTGCAG</u> ATGGAGAGCAACTACCATCC    | <i>PstI</i>    |
| <i>ZjWRKY75-R</i> | TTT <u>AGGCCT</u> CCGGAACATTGGGCTACT      | <i>StuI</i>    |
| <i>ZjAZF2-F</i>   | TTT <u>CTGCAG</u> ATGGCGGTAGACGCGATCAT    | <i>PstI</i>    |
| <i>ZjAZF2-R</i>   | TTT <u>AGGCCT</u> GGCCGGGATCATGAGCCG      | <i>StuI</i>    |
| <i>ZjNAC1-F</i>   | TTT <u>CTGCAG</u> ATGTCGATGAGTTTCGTGAG    | <i>PstI</i>    |
| <i>ZjNAC1-R</i>   | TTT <u>AAGCTT</u> GAAAGTGATTCATCCATGTAG   | <i>HindIII</i> |
| <i>ZjNAC083-F</i> | TTT <u>ACTAGT</u> ATGGACGCGAAGGAGGTGGT    | <i>SpeI</i>    |
| <i>ZjNAC083-R</i> | TTT <u>AGGCCT</u> CGCGCAGCCTCCGCTGGTGGTGT | <i>StuI</i>    |
| <i>ZjARF1-F</i>   | TTT <u>CTGCAG</u> ATGGCCGCGCCGATGGAGGTGT  | <i>PstI</i>    |
| <i>ZjARF1-R</i>   | TTT <u>AGGCCT</u> ATCAGATGGTGAGTTTACAG    | <i>StuI</i>    |
| <i>ZjPIL5-F</i>   | TTT <u>CTGCAG</u> ATGGATGGTAAGGCGAGGTC    | <i>PstI</i>    |
| <i>ZjPIL5-R</i>   | TTT <u>AGGCCT</u> AACTCCATTAGTAGGTGGCA    | <i>StuI</i>    |
| <i>ZjHB2-F</i>    | TTT <u>ACTAGT</u> ATGATGGAGAGGGCAGATGA    | <i>SpeI</i>    |
| <i>ZjHB2-R</i>    | TTT <u>AGGCCT</u> GCTGCTGGCAAGCGACTGCA    | <i>StuI</i>    |
| <i>ZjPCAP1-F</i>  | TTT <u>GGACTT</u> CATGTATTGCATATCGTTTA    | <i>BamHI</i>   |
| <i>ZjPCAP1-R</i>  | TTT <u>AGGCCT</u> GGCTGGAAACGAGGCCAAAT    | <i>StuI</i>    |

R.E.\*: restriction enzyme site

**Table 2. List of PCR primers of genes that used for qRT-PCR**

| Gene ID          | Forward Sequence (5' to 3') | Reverse Sequence (5' to 3') | DEG Type |
|------------------|-----------------------------|-----------------------------|----------|
| <i>Zj_G08090</i> | AGAGATCACGCAAGAAATCCAT      | CTGCGCCACTAATAAGATGTTG      | Specific |
| <i>Zj_G12647</i> | GGAATTCAGCAAGTCAAACCTCC     | TCGATCTCTGGTCTTTTTCCTC      | Specific |
| <i>Zj_G10221</i> | CTGGTATTGAGCCTTACCTTGG      | ACAGATTTTGCACGACAATCAC      | Specific |
| <i>Zj_G26206</i> | TATTTGCATGAGAGGTTGATCG      | CAACTCTGCGATGTTCTCTACG      | Specific |
| <i>Zj_G05196</i> | TATCATCAGGGCGAAGCTTATT      | CAGGAGGTAAAACAGCCAAGTC      | Specific |
| <i>Zj_G31160</i> | GAATTCACGAACTCTGCCTCTT      | AGCACTGGATCCATCATTCTTCT     | Specific |
| <i>Zj_G07262</i> | AAAGAGAGAGATGCTGGTGGAG      | CATATTGGAACGACACAATGCT      | Common   |
| <i>Zj_G05600</i> | TTCATGTGAGAGTTGGACCTGT      | TACATATATTGGGACGGCATGA      | Common   |
| <i>Zj_G17168</i> | ACGTTTCGCTGGTTGTATCTTT      | CTCAGCAACTGGATAAGGGTTC      | Common   |
| <i>Zj_G02756</i> | TGCTTCAGGGGAGCTACTACAT      | TCCCAAACAAACAGAATCACAC      | Common   |
| <i>Zj_G31834</i> | CTGTTGCTTGTCCAACCTCTACG     | TGTAGAGGGGTTAATGGATGCT      | Common   |
| <i>Zj_G24986</i> | TTGGGTTGGTCATTAGACTGTG      | ACAGGCACCACTTCTCATTCT       | Common   |
| <i>Zj_G27885</i> | TTAGTCGTGTTGGATTGCTTG       | TCGACTGAACCAATCAATGAAG      | Common   |
| <i>Zj_G04249</i> | CCTGTACGGCACTTAGGACTTC      | TACGTGCGACATACTGCTTTCT      | Common   |
| <i>Zj_G06230</i> | GAATTCGGTATGGAAGGACAAG      | TGTGTCAACATTGTAGCTGCTG      | Common   |
| <i>Zj_G21399</i> | AATCAGGAGGGCTAACAGACAA      | ATGGTAAATGGGCTATTGTTGG      | Common   |
| <i>Zj_G13346</i> | CAGGCCTATTGCTACTCTGCTT      | TTCCGATCCAAAATAACTTGCT      | Common   |
| <i>Zj_G29569</i> | CTTGAGGTAGACCCGCTATAA       | GACTAGTCAGTCGTGCTTGCAT      | Common   |
| <i>Zj_G23156</i> | AATTAGCATCGCAAGAGAGAGC      | TGGACAAGGATCAGGTAGCAAT      | Common   |
| <i>Zj_G03446</i> | GAGCTTGGCTTTGATTAGCAGT      | ACCATATCCAGCTGCTTTTCTC      | Common   |
| <i>Zj_G09725</i> | CAATGATGTTTCCAGGTGCTTA      | ATTTGACCTAGGCTTTGAGCTG      | Common   |
| <i>Zj_G21753</i> | GAGGCGAAGACTTGAGACAAC       | GGGACCGAAGGAGTGATAAATA      | Common   |
| <i>Zj_G23791</i> | CTCCGTAGACTTTGGCTCAGAT      | TTGCATAATTACCTTGGTGCAG      | Common   |
| <i>Zj_G07719</i> | CAGGAGTGCTACAAAGGCTTCT      | TTCTCGTTCACCTCTCTAAGG       | Common   |

## RESULTS

### **Preparation of leaf samples for comparative transcriptome analysis of age-, dark- and salt-induced senescence in *Z. japonica***

Leaf senescence is an age-dependent process that is also influenced by a variety of senescence-inducing factors, such as darkness and salt (Jehanzeb et al., 2017). Dark and salt have been widely used for a senescence assay by reflecting starvation and abiotic stress (Dong et al., 2021). Although molecular and physiological responses in various senescence conditions are similar, but their molecular senescence responses are specifically diversified at initial senescence stage. To understand the unique and common molecular mechanisms underlying various senescence responses in *Z. japonica*, I attempt to perform a comparative transcriptome analysis of age-, dark-, and salt-induced senescence responses. In this regard, temporal changes in chlorophyll contents, a typical indicator of senescence, were monitored during senescence that are triggered by age, dark, and salt (Figure 1A and 1D). Leaves at nearly 80% of the chlorophyll levels relative to their initial value in each senescence condition were considered in early senescence stage. For age-induced senescence, chlorophyll contents in 4<sup>th</sup> leaves were monitored at 4-day intervals from emergence along aging. Since chlorophyll levels in leaves at DAE 21 reached to the maximum chlorophyll level along aging, DAE21 leaves were considered at the mature green (MG) stage, the reference for age-induced senescence and were also used as the starting materials for dark- or salt-induced senescence assay (see methods for details). Chlorophyll levels in leaves gradually dropped along aging (Data not shown) and DAE 57 leaves contained

76% (around 80%) chlorophyll levels relative to those in DAE 21 leaves (referred as MG) (Figure 1C). DAE 57 (referred as SS) and DAE 21 leaves were selected as age-induced senescence and control samples for transcriptome analysis.

In dark- and salt-induced senescence, DAE 21 leaves were incubated in MES buffer under darkness and in MES buffer containing 150 mM salt in light, respectively, and their chlorophyll levels were monitored and compared with those levels kept in MES buffer in light along days of treatments. Leaves at 4 days after treatment (DAT) in dark- and salt- senescence condition contains 80% and 78% of chlorophyll levels relative to those of DAT 4 leaves in MES buffer under light and were selected as dark- and salt-induced senescence samples (referred as DARK and SALT, respectively) and controls (referred as Control-light) for transcriptome analysis (Figure 4D).

Leaves at 4 days after treatment (DAT) contains with chlorophyll levels at 80% of the initial value (named as DARK and SALT) and DAT 4 leaves in MES buffer solution under light were selected as controls (named as Control-light) for transcriptome analysis. In addition, for molecular validation of senescence responses in the senescence and control leaves selected, expression of *ZjSGR*, *COR410*, and *DREB1*, known as stress associated genes in *Z. japonica* (Kidokoro et al., 2015; Teng et al., 2016b; Li et al., 2019) was examined through qRT-PCR analysis. Transcript levels of *ZjSGR*, *COR410*, and *DREB1* increased preferentially in AGE, SALT, and DARK samples relative to their appropriate controls (MG and Control-light), respectively (Figure 1E and 1F), indicating that samples for transcriptome analysis have differential molecular responses reflecting each senescence condition and

differential molecular responses are involved in age-, salt- and dark-induced conditions as reported previously.



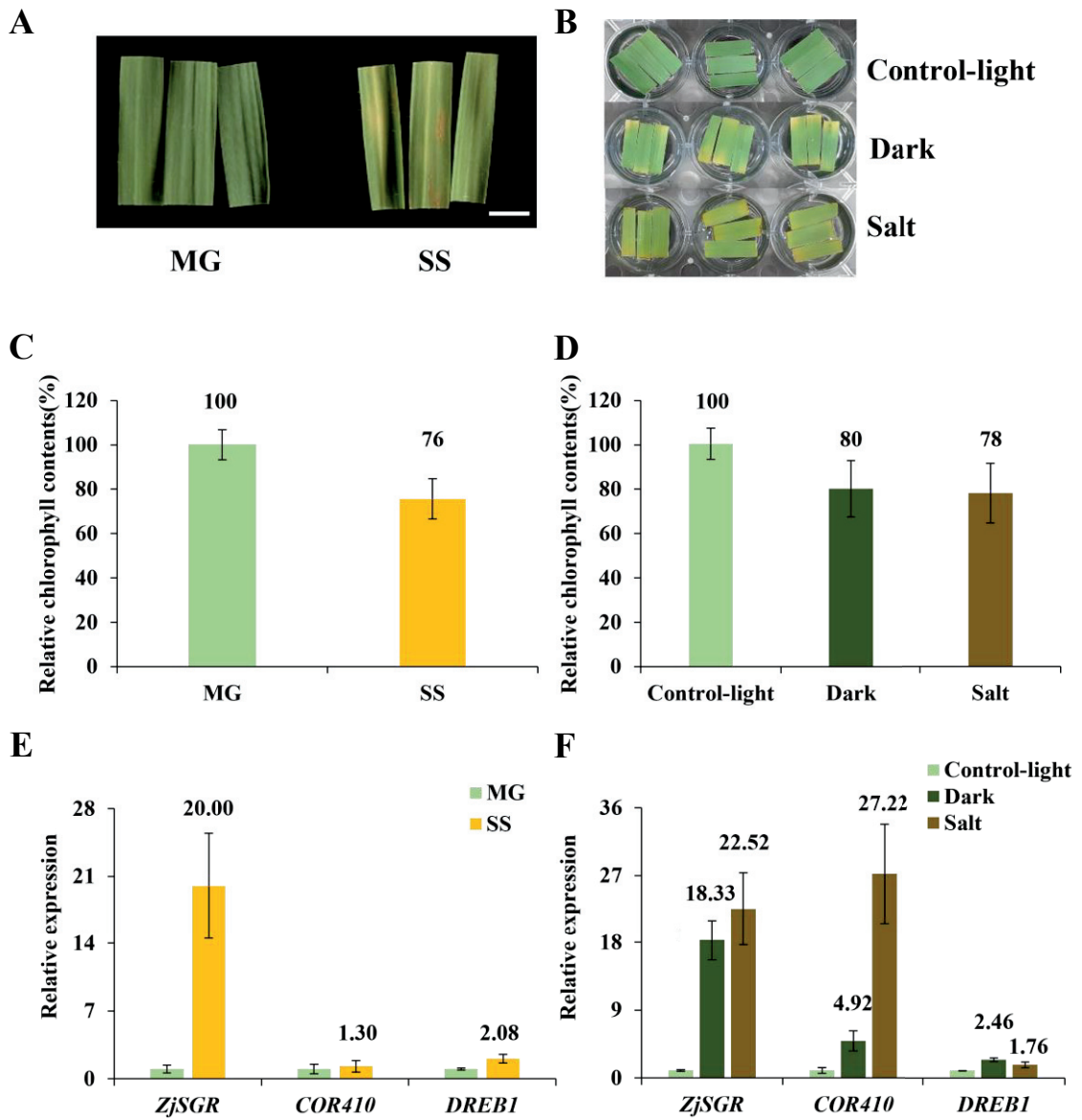


**Figure 1. Preparation of leaf samples for comparative transcriptome analysis of age-, dark- and salt-induced senescence in *Z. japonica*.**

**(A, C, E)** For age-induced senescence, the leaf fragments at DAE 21 and 57 were harvested as samples at mature green (MG) and senescence stage (SS) for transcriptome analysis, respectively. **(B,D,F)** For dark- or salt-induced senescence, the leaf fragments at DAE21 were placed in 3 mM MES buffer kept in light (Control-light; control-light for dark and salt), wrapped in aluminum foil (Dark; for dark) or in the MES buffer containing 150 mM salt (Salt; for salt), and leaf fragments at DAT4 was harvested as samples at mature green (MG) and senescence stage (SS) for transcriptome analysis. The 4<sup>th</sup> leaves emerged from a bud were cut at the indicated days of leaf emergence (DAE) into three pieces and the middle part was used for senescence assay. Representative pictures of the leaf fragments in MG and SS in age-induced senescence **(A)** and those in dark- and salt-induced senescence as well as control-light **(B)**. Leaf fragments of SS **(C)**, and Dark and Salt **(D)** contained 75-80% of chlorophyll content relative to those of each control, which is a typical indication of early senescence. Data represent mean  $\pm$  SE (n=6). Senescence-related gene expression in MG and SS leaf fragments **(E)**, and in Control-light, Dark, and salt **(F)** leaf fragments. Gene expression was determined by qRT-PCR by normalization against *zjACT2* expression. Data represent mean  $\pm$  SE (n=3).

## **Transcriptomic comparison of age, dark, and salt-induced senescence**

To explore the molecular basis of age, dark, and salt-induced leaf senescence in *Z. japonica*, I performed mRNA sequencing analysis for a total of five biological samples (MG, AGE, Control-light, DARK, and SALT) with three biological replicates. These samples were for three comparison sets with age- (MG vs AGE), dark- (Control-light vs DARK), and salt- (Control-light vs SALT) induced senescence. Library construction and subsequent sequencing were performed in total 15 samples and a total of 124.1 Gb of high-quality clean data was obtained.

The GC content of raw reads ranged from 51.8% to 53.4% in different libraries, with Q30 percentages exceeding 96.5% (Table 3). 73.1-95.3 % of the total clean reads from each sample were well-mapped to the available *Z. japonica* reference genome (Table 4), but the ratio of transcript matching was relatively low with an average matching rate of approximately 75.2% (Lin et al., 2020). Visual exploration of the mapped reads on the *Z. japonica* genome annotation revealed that such a low mapping rate on the transcripts was due to inaccurate *Z. japonica* transcript annotation. To obtain accurate expression data for each gene in *Z. japonica*, its genome annotation was rebuilt as a GTF file with new gene identification (ID) system, based on our RNA-seq data. The comparison table between new and old gene IDs in *Z. japonica* genome was provided as the dataset (Dataset 1). Accordingly, the mapping ratio of reads on transcripts with new genome annotation increased to 88.8 to 95.4% (Table 4). Next, gene expression levels in all *Z. japonica* genes were calculated as FPKM values and normalized among the 15 samples. 68383 genes, 52.6 % of nuclear genes were expressed in *Z. japonica* leaves in our conditions. I further performed the principal

component analysis (PCA) with expressed genes in each condition to validate the quality of our samples (Dong et al., 2022). PCA analysis for 15 biological samples indicated that transcriptomic profiles of *Z. japonica* leaves in each senescence condition showed close clusters among the same biological samples relative to others (Figure 2), implying a reliability of our RNA-seq data to reflect each biological condition.

**Table 3. Raw data statistics**

| Samples         | Total read base | Total reads | QC(%) | Q30(%) |
|-----------------|-----------------|-------------|-------|--------|
| Control-light-1 | 9,007,616,926   | 89,184,326  | 53.3  | 96.6   |
| Control-light-2 | 8,018,001,150   | 79,386,150  | 52.8  | 96.4   |
| Control-light-3 | 9,013,979,724   | 89,247,324  | 53.0  | 96.6   |
| SALT-1          | 8,470,380,554   | 83,865,154  | 51.0  | 96.3   |
| SALT-2          | 7,692,189,694   | 76,160,294  | 51.8  | 96.6   |
| SALT-3          | 8,574,612,150   | 84,897,150  | 52.4  | 96.5   |
| DARK-2          | 8,814,549,770   | 87,272,770  | 52.2  | 96.5   |
| DARK-3          | 8,795,829,824   | 87,087,424  | 52.5  | 96.5   |
| DARK-4          | 8,370,741,428   | 82,878,628  | 52.3  | 96.5   |
| MG-1            | 7,220,428,794   | 71,489,394  | 53.0  | 96.5   |
| MG-2            | 7,579,553,080   | 75,045,080  | 53.3  | 96.6   |
| MG-3            | 7,418,014,892   | 73,445,692  | 53.4  | 96.6   |
| AGE-1           | 7,535,835,028   | 74,612,228  | 52.2  | 96.2   |
| AGE-2           | 9,036,141,750   | 89,466,750  | 53.1  | 96.6   |
| AGE-3           | 8,987,696,090   | 88,987,090  | 53.2  | 96.6   |

Total read bases (Total number of bases sequenced) = Total reads x Read length; Total reads: Total number of reads; GC (%): GC content; Q30 (%): Ratio of bases that have phred quality score greater than or equal to 30.

**Table 4. Mapping status of 15 samples**

| Samples         | Total transcripts No. | Transcript matching ratio(%) | Transcript No. with new annotation file | Transcript matching ratio with new annotation file(%) |
|-----------------|-----------------------|------------------------------|---|---|
| Control-light-1 | 35,662                | 76.3                         | 33,878                                  | 94.1  |
| Control-light-2 | 35,612                | 76.7                         | 33,831                                  | 94.0  |
| Control-light-3 | 35,936                | 74.5                         | 34,139                                  | 94.9  |
| SALT-1          | 36,050                | 73.6                         | 34,247                                  | 95.2  |
| SALT-2          | 35,693                | 73.9                         | 33,908                                  | 94.2  |
| SALT-3          | 34,982                | 73.8                         | 33,181                                  | 92.2  |
| DARK-2          | 36,136                | 75.1                         | 34,329                                  | 95.4  |
| DARK-3          | 35,902                | 76.4                         | 34,106                                  | 94.8  |
| DARK-4          | 35,332                | 74.3                         | 33,565                                  | 93.3  |
| MG-1            | 35,530                | 80.7                         | 33,753                                  | 93.8  |
| MG-2            | 34,891                | 75.2                         | 33,146                                  | 92.1  |
| MG-3            | 33,645                | 72.5                         | 31,962                                  | 88.8  |
| AGE-1           | 35,211                | 79.7                         | 33,450                                  | 93.0  |
| AGE-2           | 34,030                | 74.4                         | 32,587                                  | 90.6  |
| AGE-3           | 34,195                | 71.5                         | 32,485                                  | 90.3  |

Transcript matching ratio was compared when transcript annotation were published (2<sup>nd</sup> and 3<sup>rd</sup> columns) or a new transcript annotation (two right columns, highlighted in yellow) generated from the RNA-seq data.

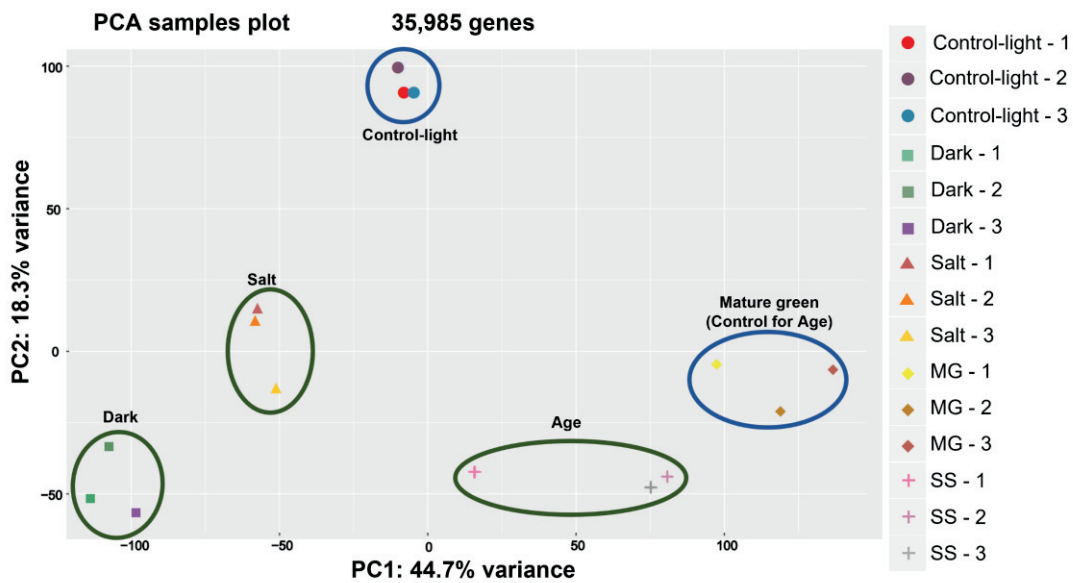


**Figure 2. PCA analysis for transcriptome responses in *Z. japonica* leaves under the different senescence conditions.** For dark- and salt-induced senescence condition, 21-d-old *Z. japonica* leaves grown in the soil were detached and treated with dark (Dark) or salt (Salt) for 4 d, along with light (Control-light; Control for Dark and Salt). For age-induced senescence condition, 21- and 57-d-old mature green (Mature green; Control for Age) and senesced leaves (Age) were harvested, respectively. Three biological samples per each condition were used. RNA-seq was performed using total RNAs extracted from each sample. The PCA analysis was performed with expression profiles in 35985 genes using PCAGO. PC1 and PC2 explains 44.7% and 18.5% of the variance.

## **Functional characterization of transcriptomic responses in age-, dark-, and salt-induced senescence**

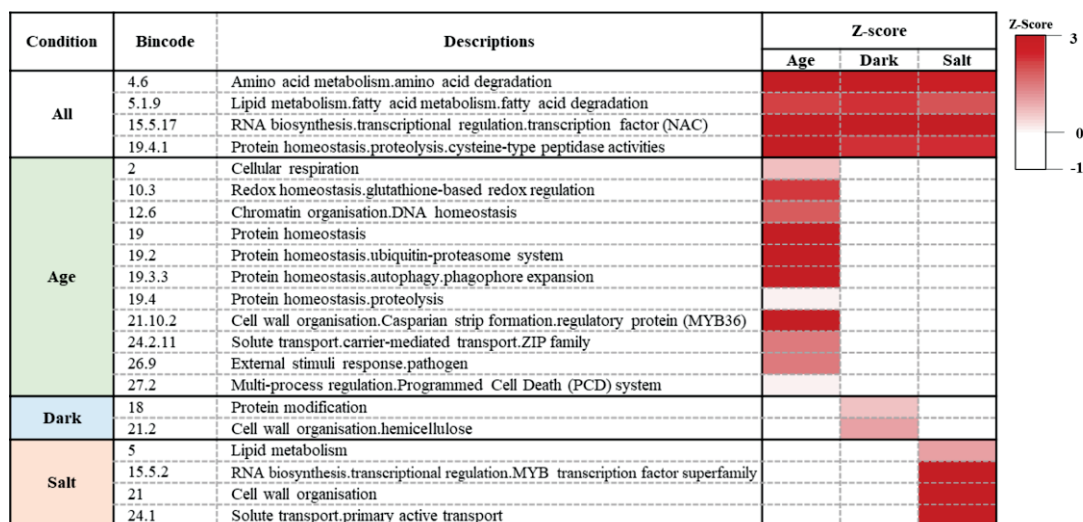
To comprehend and dissect the biological processes that occurs during senescence transcriptome, enrichment analysis of functional categories with defined gene sets were performed with transcriptomic profiles from expressed genes in each senescence condition.

I loaded the data into Pageman for visualization of MapMan functional categories and analyse the relationship between the enriched transcripts of different senescence-induced conditions and their biological significance. This analysis condensed the 35985 expressed genes into approximately 5257 categories. Bincode and  $|Z\text{-Score}| > 1.96$  were used to further compress these categories, whereas categories that did not demonstrate significantly distinct changes were removed (Figure 3), with red BINs significantly up-regulated in comparison to the rest of the array, and blue BINs down-regulated. The research shows that transcriptomes that co-respond to different senescence-inducing conditions have a significant impact on certain biological processes. Genes involved in the degradation of proteins and lipids as well as the synthesis of some transcription factor families were among those found to be up regulated (Figure 3A). The most noticeable physiological aspect of leaf senescence is leaf yellowing, the photosynthesis response is the biological process of down-regulated gene enrichment (Figure 3B). MapMan showed the effect of different senescence-inducing conditions on more distinct processes. Redox regulation and protein degradation were the biological processes that were most enriched under age-induced senescence conditions, and within protein degradation, autophagy and



ubiquitin-associated pathways were the major up-regulated categories. In contrast, genes related to gibberellin (GA) synthesis were significantly down regulated, which is consistent with previously reported that GA delayed the onset of leaf senescence and the level of GA in mature leaves was reduced (Akhtar et al., 2019). Genes involved in hemicellulose synthesis were increased during dark-induced senescence, whereas genes involved in protein biosynthesis were downregulated. Furthermore, under conditions of salt-induced senescence, salt-induced changes in genes associated to lipid metabolism as well as multiple transcription factor families were evident.

**A**



**B**

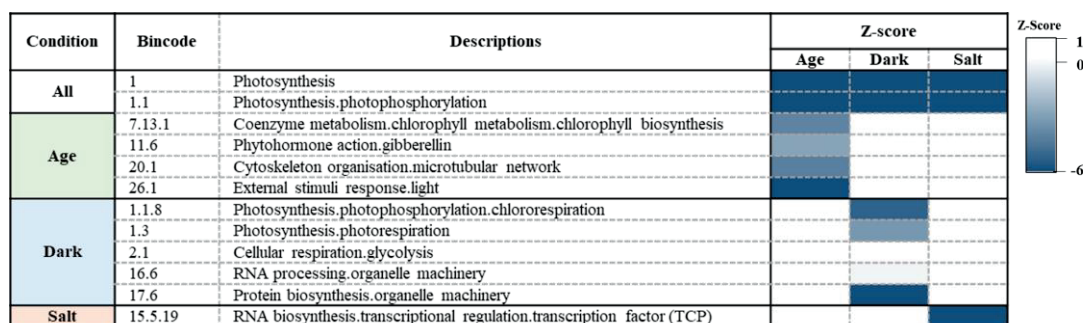


**Figure 3. Gene set enrichment analysis for transcriptome profiles in each senescence condition.** Sequence homology-based gene categorization was established with new *Z. japonica* gene IDs using Mercator. Transcriptome profiles in each senescence conditions were loaded using the MapMan and the functional categories with significant increased (A) and decreased (B) expression profiles were shown in age-, dark- and salt-induced senescence.

## Identification of differentially expressed genes

Among the 35985 expressed genes, differentially expressed genes were identified using a pair-wise comparison of gene expression in each senesced and control condition, with the selection threshold of an adjusted p-value of  $<0.05$  and  $|\text{Log}_2\text{Fold-Change}| > 1$ .

In age-, dark-, and salt-induced senescence responses, a total of 1397, 8437, and 6328 genes (3.9%, 23.4%, and 17.6% of the total expressed genes [35985 genes], respectively) were reported as significant DEGs. These included 995, 4287 and 3675 upregulated genes (16.9%, 73.0%, and 62.6% of 5876 up-regulated genes [UP]) and 402, 4150 and 2653 down-regulated genes (7.4%, 76.5%, and 48.9% of 5423 down-regulated genes [DOWN], respectively) in age-, dark- and salt-induced senescence. 173, 1920, and 1335 DEGs in the UP group and 152, 2530, and 1091 DEGS in the DOWN group (Figure 4) responded specifically in age-, dark- and salt-induced senescence responses, respectively. It is noted that a higher number of DEGs were obtained in senescence triggered by dark and salt than age. Overall, more genes were up-regulated than down-regulated under each senescence-inducing condition. DEG Venn diagrams show the number and identification of shared DEGs between two or more senescence-inducing conditions, as well as DEGs particular to each condition. Core DEGs (633 UP and 132 DOWN) that co-respond to age-, dark-, and salt-inducing senescence conditions were identified (Figure 4A and 4B), indicating that each senescence condition during senescence may use a shared set of genes during the

senescence process, and these DEGs may potentially be associated in the occurrence and development of leaf senescence in *Z. japonica*.

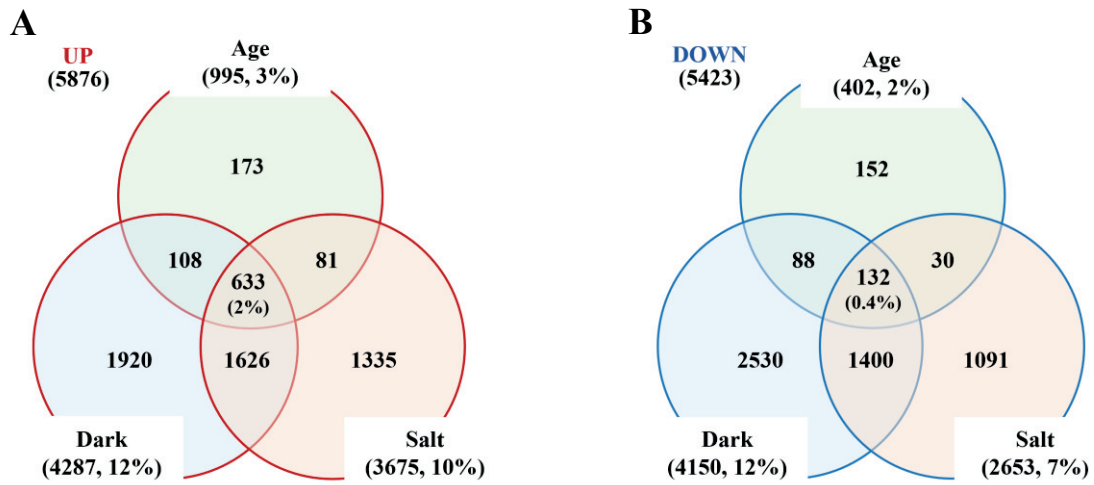


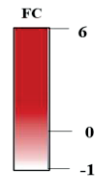
**Figure 4. Comparison of the number of differentially expressed genes in different senescence-induced conditions.** (A) Venn diagrams of the up-regulated genes (UP) on age, dark, and salt-induced senescence conditions. (B) Venn diagrams of down-regulated genes (DOWN) on age, dark, and salt-induced senescence condition. The differentially expressed genes (DEGs) were selected by the cutoff with  $\log_2(\text{Fold Change}) > 2$  and significance adjusted p-value of  $< 0.05$  with nbinomWaldTest using DESeq2 per comparison pair.

## **Validation of qRT-PCR of differentially expressed genes in each senescence condition**

Since endogenous factors (such as age, ethylene, jasmonic acid, salicylic acid, abscisic acid, and cytokinin) and exogenous factors (such as UV radiation, dark, salt and temperature) affect leaf senescence through different gene network (Zhang and Zhou, 2013), molecular markers specifically responsive in each senescence condition are highly demanded. I identified differentially expressed genes responsive specifically for age-, dark-, and salt-induced senescence. These were selected based on three criteria: 1) gene expression levels (FPKM > 1), 2) significantly responsive to each senescence condition (Adjusted-P < 0.05 & |log<sub>2</sub>fold change| > 2), and 3) senescence responsiveness of their Arabidopsis homologous genes. 20 up- and 20 down-regulated DEGs were selected specifically responsive DEGs (sDEGs) in each condition (Figure 5). Among them, expression profiles of one up-regulated and one down-regulated sDEG in each condition (UP: *Zj\_G01458* and DOWN: *Zj\_G12647* for AGE; UP: *Zj\_G10221* and DOWN: *Zj\_G26206* for DARK; UP: *Zj\_G05196* and DOWN: *Zj\_G31160* for SALT) were validated by qRT-PCR using independent biological samples from those used for RNA-seq analysis. Expression of these six genes selected as sDEGs was increased or decreased in each designated senescence condition as expected in RNA-seq analysis (Figure 6A and 6C), although some of genes including *Zj\_G12647*, *Zj\_G05196*, and *Zj\_G31160* showed opposite responsiveness in other senescence conditions. These results indicate that these genes examined can be used as senescence markers to dissect senescence inducing condition. Further, these convinced the reliability of the transcriptome sequencing data in this study.

A

| Up                       | Gene ID   | Gene description                                     | AGI          | AtSymbol     | Age | Dark | Salt |
|--------------------------|-----------|--|--------------|--------------|-----|------|------|
| A<br>G<br>E<br>(20)      | Zj_G08048 | Unidentified   | Unidentified | Unidentified |     |      |      |
|                          | Zj_G07281 | Os01g0855700 protein (Fragment)                      | AT2G40000    | HSPRO2       |     |      |      |
|                          | Zj_G11064 | E3 ubiquitin-protein ligase ATL6                     | AT3G05200    | ATL6         |     |      |      |
|                          | Zj_G20779 | Putative LRR receptor-like serine                    | AT1G74360    | AT1G74360    |     |      |      |
|                          | Zj_G31208 | Aa trans domain-containing protein                   | AT5G41800    | AT5G41800    |     |      |      |
|                          | Zj_G01458 | Glutamate decarboxylase                              | AT5G17330    | gad          |     |      |      |
|                          | Zj_G08090 | Jacalin-type lectin domain-containing protein        | AT1G73040    | AT1G73040    |     |      |      |
|                          | Zj_G27703 | Uncharacterized protein                              | AT5G51060    | RHD2         |     |      |      |
|                          | Zj_G03474 | Uncharacterized protein (Fragment)                   | AT1G63440    | HMA5         |     |      |      |
|                          | Zj_G00315 | Unidentified   | AT4G27250    | AT4G27250    |     |      |      |
|                          | Zj_G19883 | Unidentified   | AT1G77450    | anac032      |     |      |      |
|                          | Zj_G20290 | DUF4220 domain-containing protein                    | AT5G45540    | AT5G45540    |     |      |      |
|                          | Zj_G11342 | p-glycoprotein 1                                     | AT2G36910    | ABCB1        |     |      |      |
|                          | Zj_G22707 | Uncharacterized protein                              | Unidentified | Unidentified |     |      |      |
|                          | Zj_G23505 | Glycosyltransferase                                  | AT4G01070    | GT72B1       |     |      |      |
|                          | Zj_G30574 | Unidentified   | AT2G32270    | Zip3         |     |      |      |
|                          | Zj_G29621 | Oligopeptide transporter 1-like                      | AT5G55930    | OPT1         |     |      |      |
|                          | Zj_G22572 | Nodulin-like domain-containing protein               | AT2G39210    | AT2G39210    |     |      |      |
|                          | Zj_G11906 | Uncharacterized protein                              | AT5G48930    | Hct          |     |      |      |
|                          | Zj_G16657 | Unidentified   | Unidentified | Unidentified |     |      |      |
| D<br>A<br>R<br>K<br>(20) | Zj_G03922 | Uncharacterized protein                              | AT5G54190    | porA         |     |      |      |
|                          | Zj_G10550 | Glutamate dehydrogenase                              | AT5G18170    | gdh1         |     |      |      |
|                          | Zj_G12735 | Putative WRKY transcription factor 53                | AT4G23810    | WRKY53       |     |      |      |
|                          | Zj_G26956 | ANK_REP_REGION domain-containing protein             | AT4G03500    | AT4G03500    |     |      |      |
|                          | Zj_G29642 | Homeobox domain-containing protein                   | AT4G40060    | ATHB16       |     |      |      |
|                          | Zj_G15756 | Protein kinase domain-containing protein             | AT3G01490    | AT3G01490    |     |      |      |
|                          | Zj_G10221 | Phytochrome  | AT1G09570    | phyA         |     |      |      |
|                          | Zj_G04252 | DDE Tnp4 domain-containing protein (Fragment)        | AT5G12010    | AT5G12010    |     |      |      |
|                          | Zj_G06436 | Uncharacterized protein                              | AT2G25490    | EBF1         |     |      |      |
|                          | Zj_G29777 | Auxin-responsive protein                             | AT2G22670    | IAA8         |     |      |      |
|                          | Zj_G09662 | Peroxidase   | AT4G37530    | AT4G37530    |     |      |      |
|                          | Zj_G22220 | AP2/ERF domain-containing protein                    | AT1G78080    | RAP2.4       |     |      |      |
|                          | Zj_G05736 | Xyloglucan endotransglucosylase/hydrolase            | AT1G32170    | XTR4         |     |      |      |
|                          | Zj_G06001 | Uncharacterized protein (Fragment)                   | AT5G61380    | TOC1         |     |      |      |
|                          | Zj_G20892 | Unidentified   | AT1G26800    | AT1G26800    |     |      |      |
|                          | Zj_G13969 | Auxin efflux carrier component                       | AT1G73590    | PIN1         |     |      |      |
|                          | Zj_G01212 | Protein-serine/threonine phosphatase                 | AT2G30020    | AT2G30020    |     |      |      |
|                          | Zj_G08551 | Transcription factor APG-like isoform X1             | AT1G09530    | pi3          |     |      |      |
|                          | Zj_G34728 | Unidentified   | AT2G30020    | AT2G30020    |     |      |      |
|                          | Zj_G12460 | NAC domain-containing protein                        | AT2G33480    | ANAC041      |     |      |      |
| S<br>A<br>L<br>T<br>(20) | Zj_G05754 | Uncharacterized protein                              | AT1G32450    | NRT1.5       |     |      |      |
|                          | Zj_G13076 | MFS domain-containing protein (Fragment)             | AT3G13050    | AtNiaP       |     |      |      |
|                          | Zj_G31188 | Sl707066f01  | AT1G17745    | PGDH         |     |      |      |
|                          | Zj_G31237 | Mitogen-activated protein kinase                     | AT2G42880    | ATMPK20      |     |      |      |
|                          | Zj_G05196 | Plasma membrane intrinsic protein 1                  | AT4G23400    | PIP1.5       |     |      |      |
|                          | Zj_G03409 | Uncharacterized protein (Fragment)                   | AT1G62660    | AT1G62660    |     |      |      |
|                          | Zj_G08150 | Uncharacterized protein                              | AT1G17350    | AT1G17350    |     |      |      |
|                          | Zj_G11015 | HVA22-like protein                                   | AT5G50720    | ATHVA22E     |     |      |      |
|                          | Zj_G01831 | Beta-amylase   | AT3G23920    | BAM1         |     |      |      |
|                          | Zj_G22238 | Uncharacterized protein                              | AT5G37810    | NIP4.1       |     |      |      |
|                          | Zj_G09388 | Uncharacterized protein                              | AT3G22600    | LTPG5        |     |      |      |
|                          | Zj_G18677 | Abhydrolase_2 domain-containing protein (Fragment)   | AT3G15650    | AT3G15650    |     |      |      |
|                          | Zj_G05468 | Annexin  | AT5G65020    | ANNAT2       |     |      |      |
|                          | Zj_G11451 | Tip4b  | AT2G25810    | TIP4.1       |     |      |      |
|                          | Zj_G26399 | Uncharacterized protein (Fragment)                   | AT1G59870    | PEN3         |     |      |      |
|                          | Zj_G10939 | Malate dehydrogenase                                 | AT3G47520    | mdh          |     |      |      |
|                          | Zj_G17918 | HMA domain-containing protein                        | AT3G06130    | AT3G06130    |     |      |      |
|                          | Zj_G05971 | Phenylalanine ammonia-lyase                          | AT2G37040    | pall         |     |      |      |
|                          | Zj_G19568 | Glyco transf 20 domain-containing protein (Fragment) | AT1G68020    | ATTPS6       |     |      |      |
|                          | Zj_G07286 | TPR_REGION domain-containing protein                 | AT2G29670    | AT2G29670    |     |      |      |



**B**

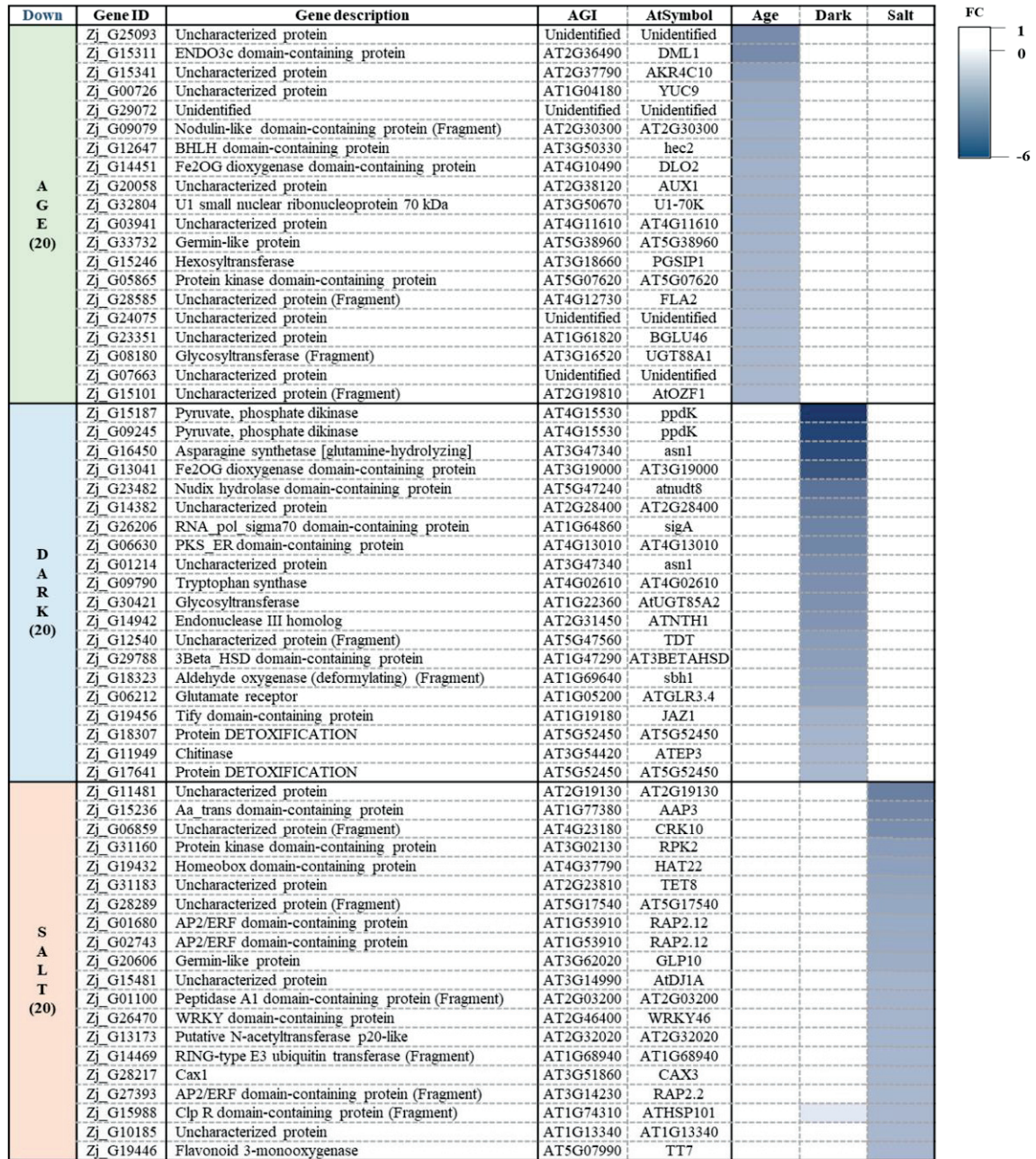


**Figure 5. Specifically responsive genes in each senescence condition.** DEGs specifically responding to dark-, salt-, age- were shown. Heatmaps for fold-changes (FC) in DEGs expression in each condition are shown. The color intensities indicate  $\text{Log}_2(\text{FC})$ . Expression heat map of up- (A) and down- (B) regulated DEGs in each senescence condition.



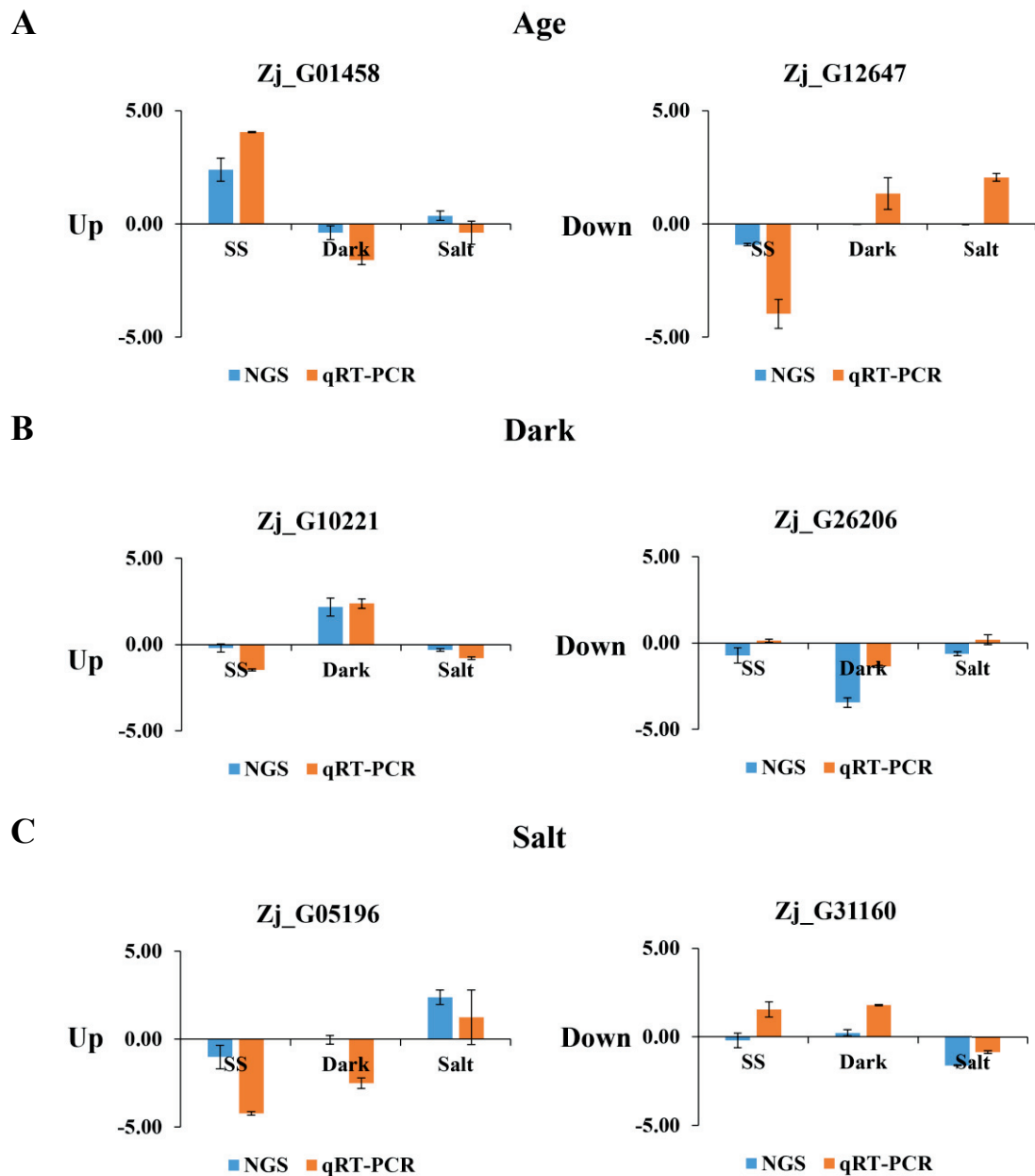


**Figure 6. qRT-PCR-based validation of DEGs that were responsive in each senescence condition through RNA-seq analysis.** (A-C) Expression profile of DEGs that were up- (left) and down (right)-regulated in each senescence condition triggered by age- (A), dark- (B), and salt (C). Samples were prepared as in Figure 1. Data represent mean  $\pm$  SE (n=3).

## Identification and expression profile of TF cDEGs

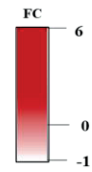
Since senescence involves transcriptional changes in thousands of genes, TFs are essential for regulating leaf senescence (Dong et al., 2022). In addition, TFs are potential gene resources for altering senescence phenotypes as shown in many studies of TFs in crop (Sekhon et al., 2012; Jan et al., 2013; Bengoa Luoni et al., 2019; Wang et al., 2021). To select gene resources that likely affect senescence, 55 up-regulated TFs and 8 down-regulated TFs that were highly responsive to senescence-inducing conditions were selected among cDEGs. Typical representative TFs family includes NAC, WRKY, bHLH, and ARF (Figure 7), which are the major families reported to be associated with senescence regulation. Most of the bHLH and ARF TFs were down-regulated, while the NAC and WRKY TF families were up-regulated. To confirm expression profiles of TF cDEGs, expression profiles of 10 up and 4 down DEGs selected were evaluated in age-, dark-, and salt-induced senescence (Figure 8). Among them, 11 out of 14 (79%) genes were confirmed with cDEG in qRT-PCR analysis and these include 9 up-regulated DEGs, including *Zj\_G23156*, *Zj\_G21399*, *Zj\_G06230*, *Zj\_G27885*, *Zj\_G24986*, *Zj\_G31834*, *Zj\_G17168*, *Zj\_G05600*, and *Zj\_G07262*, and 4 down-regulated cDEGs including *Zj\_G21753* and *Zj\_G09725*. Of note, other *Zj\_G29569*, *Zj\_G03446*, and *Zj\_G23791* were only affected in age- and dark-induced senescence.

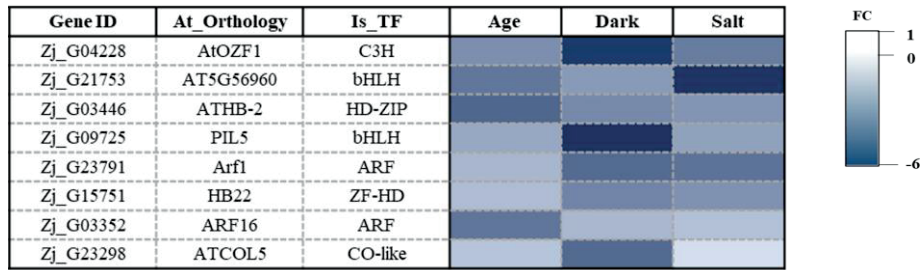
Among them, a total of five up-regulated and one down-regulated TF cDEGs as well were further investigated in a kinetic manner. Two down-regulated TF DEGs, *Zj\_G03446* and *Zj\_G23791* in age and dark-induced senescence were also included in kinetic analysis, because they might be changed in other time points. Further kinetic

analysis of these eight genes in all three conditions showed their gradual responses along senescence period except for *Zj\_G03446*, indicating a convergent role of these TFs in senescence (Figure 9). *Zj\_G03446* was also included as a regulatory group in further analysis since HB-2, Arabidopsis homologous gene of *Zj\_G03446* is known to act as senescence regulatory gene (Soledad et al., 2021). Overall, these validate the result of our presented RNA-seq analysis and provides a potential regulatory and convergent TF genes along senescence.

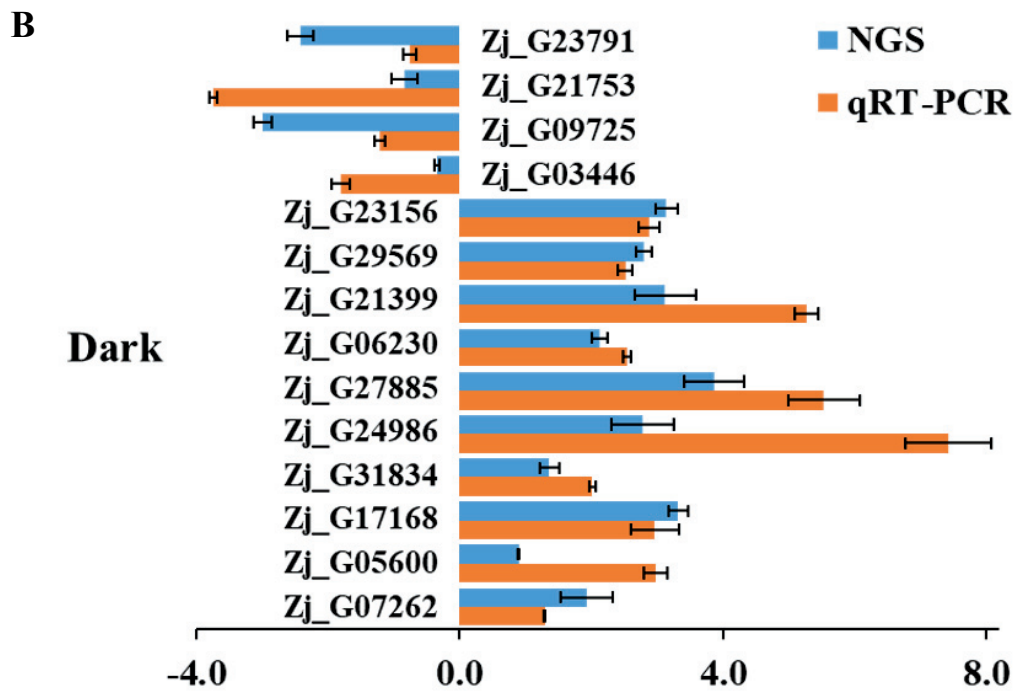
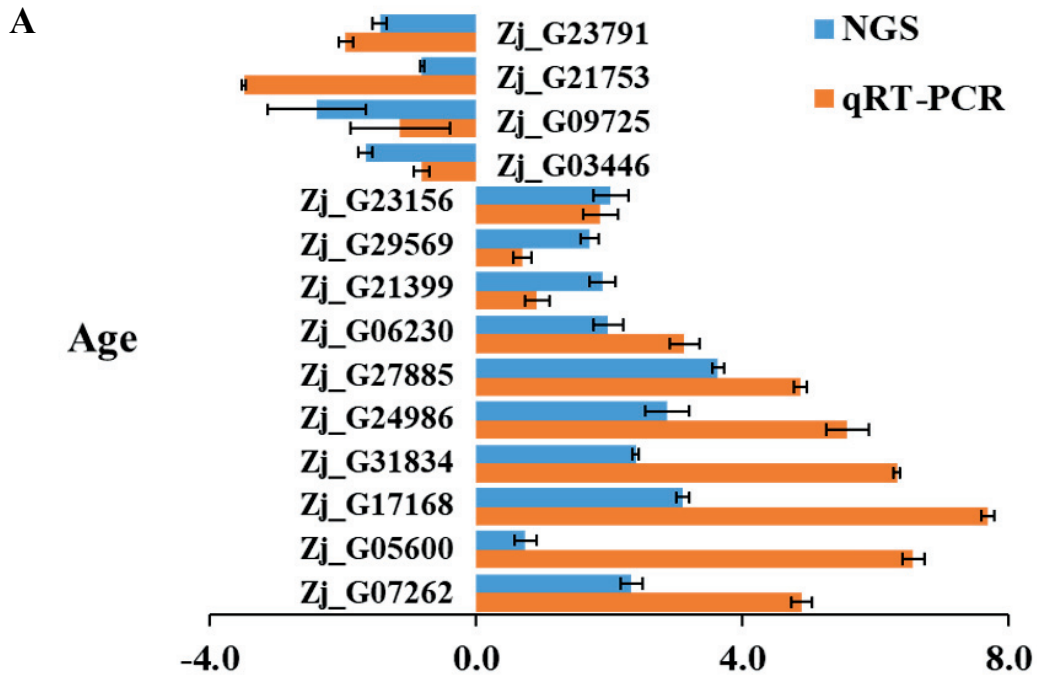
A

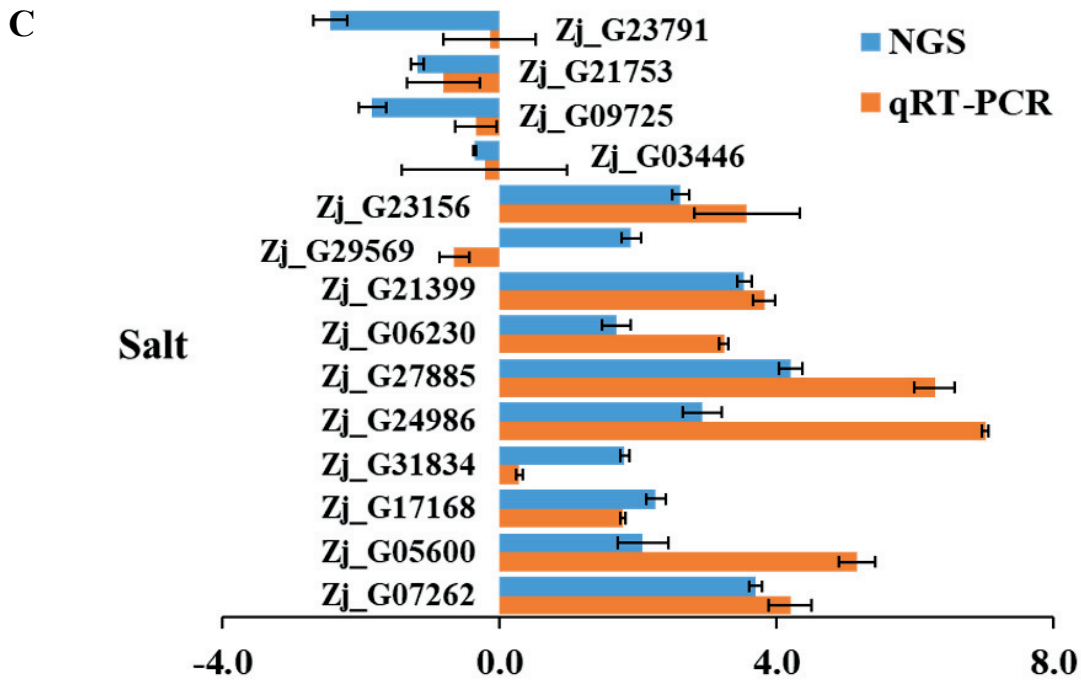
| Gene ID   | At Orthology | Is TF       | Age | Dark | Salt |
|-----------|--------------|-------------|-----|------|------|
| Zj_G04581 | NAM          | NAC         |     |      |      |
| Zj_G07262 | ABI5         | bZIP        |     |      |      |
| Zj_G06877 | WRKY49       | WRKY        |     |      |      |
| Zj_G08148 | AGL8         | MIKC        |     |      |      |
| Zj_G02310 | LBD11        | LBD         |     |      |      |
| Zj_G24986 | anac074      | NAC         |     |      |      |
| Zj_G07355 | AT3G10470    | C2H2        |     |      |      |
| Zj_G20445 | ATNAC2       | NAC         |     |      |      |
| Zj_G05600 | NF-YB6       | NF-YB       |     |      |      |
| Zj_G27885 | AZF2         | C2H2        |     |      |      |
| Zj_G25222 | anac090      | NAC         |     |      |      |
| Zj_G06089 | AP3          | MIKC        |     |      |      |
| Zj_G23364 | anac074      | NAC         |     |      |      |
| Zj_G21399 | ARF19        | ARF         |     |      |      |
| Zj_G17847 | lrp1         | SRS         |     |      |      |
| Zj_G00042 | MYR2         | G2-like     |     |      |      |
| Zj_G02353 | ZAT11        | C2H2        |     |      |      |
| Zj_G05267 | anac074      | NAC         |     |      |      |
| Zj_G01994 | AT1G76880    | Trihelix    |     |      |      |
| Zj_G16373 | MIF2         | ZF-HD       |     |      |      |
| Zj_G33286 | AT2G28710    | C2H2        |     |      |      |
| Zj_G08654 | WRKY22       | WRKY        |     |      |      |
| Zj_G21062 | ANAC087      | NAC         |     |      |      |
| Zj_G27987 | AT5G61890    | ERF         |     |      |      |
| Zj_G07011 | ANAC083      | NAC         |     |      |      |
| Zj_G02666 | ATHB40       | HD-ZIP      |     |      |      |
| Zj_G23704 | AtMYB78      | MYB         |     |      |      |
| Zj_G19408 | Unidentified | HSF         |     |      |      |
| Zj_G01295 | TRFL2        | MYB related |     |      |      |
| Zj_G06609 | Unidentified | SBP         |     |      |      |
| Zj_G08909 | ANAC002      | NAC         |     |      |      |
| Zj_G17174 | MIF2         | ZF-HD       |     |      |      |
| Zj_G30944 | MYB111       | MYB         |     |      |      |
| Zj_G17168 | NAP          | NAC         |     |      |      |
| Zj_G19854 | AHBP-1B      | bZIP        |     |      |      |
| Zj_G23156 | ANAC083      | NAC         |     |      |      |
| Zj_G01046 | anac047      | NAC         |     |      |      |
| Zj_G12641 | Unidentified | HSF         |     |      |      |
| Zj_G02162 | anac025      | NAC         |     |      |      |
| Zj_G24707 | HAT22        | HD-ZIP      |     |      |      |
| Zj_G15233 | ANAC002      | NAC         |     |      |      |
| Zj_G18994 | AT3G13040    | G2-like     |     |      |      |
| Zj_G13016 | KNU          | C2H2        |     |      |      |
| Zj_G29569 | NAC1         | NAC         |     |      |      |
| Zj_G06230 | NAC1         | NAC         |     |      |      |
| Zj_G16382 | ATNAC2       | NAC         |     |      |      |
| Zj_G33377 | AT1G76880    | Trihelix    |     |      |      |
| Zj_G06245 | AT2G40260    | G2-like     |     |      |      |
| Zj_G31834 | WRKY75       | WRKY        |     |      |      |
| Zj_G02376 | TRFL2        | MYB related |     |      |      |
| Zj_G09527 | AtGRF1       | GRF         |     |      |      |
| Zj_G16577 | AT1G29160    | Dof         |     |      |      |
| Zj_G31931 | WRKY71       | WRKY        |     |      |      |
| Zj_G00035 | AHBP-1B      | bZIP        |     |      |      |
| Zj_G19525 | ZFHD1        | ZF-HD       |     |      |      |



**B**

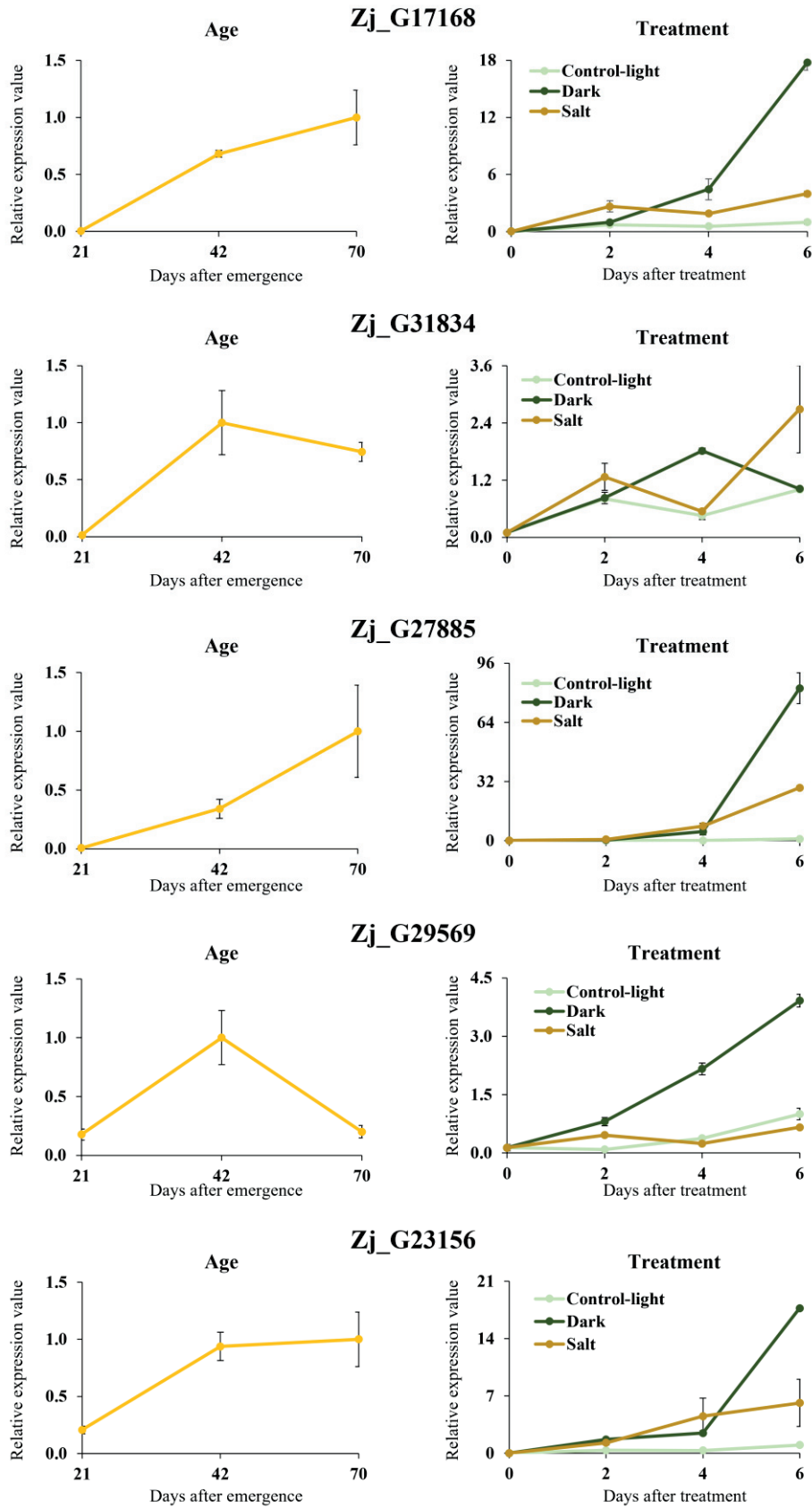
**Figure 7. Expression of *Z. japonica* TFs in response to all senescence conditions.** (A) and (B) Expression heatmap of TFs with up- (A) and down (B)-regulated expression under all senescence conditions examined. Heatmaps for fold-changes (FC) in transcription factor (TF) expression in each condition are shown. The color intensities indicate  $\text{Log}_2(\text{FC})$ .



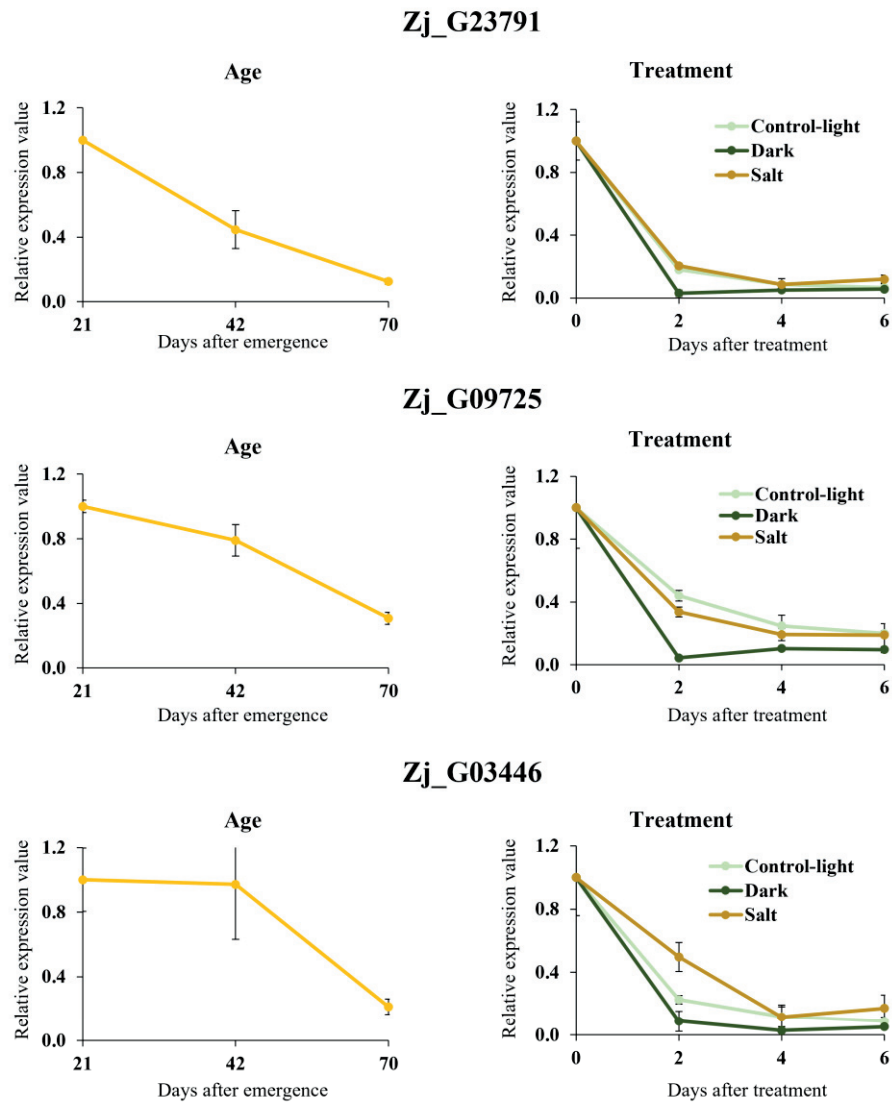


**Figure 8. qRT-PCR-based validation of TF DEGs that were responsive in all senescence condition examined through RNA-seq analysis.** (A-C) Expression profile of DEGs that were commonly responsive in age- (A), dark- (B), and salt- (C) induced senescence conditions. Samples were prepared as in Figure 1. Data represent mean  $\pm$  SE (n=3).

A





**B**

**Figure 9. Kinetic expression pattern of TF DEGs identified by RNA-seq analysis along senescence. (A) Expression of up-regulated DEGs. (B) Expression of down-regulated DEGs. Data represent the mean  $\pm$  SE (n=3). Samples were prepared as in Figure 1 but harvested in indicated age or treatment.**

## **Effect of TF candidate genes in the *Z. japonica* senescence promoters in a protoplast-mediated transient expression system**

Transcriptome analysis and further qRT-PCR experiments revealed that five up-regulated and three down-regulated transcription factors are highly responsive to all senescence condition, indicating a possibility that they might be involved in regulation of leaf senescence in *Z. japonica*. To evaluate their regulatory actions of these candidate in leaf senescence, the protoplast-based senescence assay using the reporter of senescence promoters was performed (Doan et al., 2022). Since these candidate genes are members of known TFs (Figure 10A), the proper expression of TF protein tagged eGFP was confirmed by their nuclear localization in Arabidopsis protoplasts (Figure 10B).

To perform the protoplast-based senescence assay using the *Z. Japonica* promoters, *ZjPCAP* and *ZjSGR* that respond with early-inducing and late-inducing patterns to all senescence conditions, respectively, were used as reporter promoters. Luciferase reporter driven by *ZjPCAP* and *ZjSGR* (*ZjPCAP-LUC* and *ZjSGR-LUC*) were co-transfected with GFP-fused TF effector plasmids as well as GFP as a control in the Arabidopsis protoplasts and their time-series luminescence levels were examined and compared. *ZjPCAP-LUC* and *ZjSGR-LUC* expression, in co-transfecting with the GFP control, was significantly induced, but with different patterns: *ZjPCAP-LUC* exhibited an earlier peak followed by a gradual reduction while *ZjSGR-LUC* did a later peak but with a continuous steady level. When *ZjNAP-GFP* and *ZjNAC1-GFP* were expressed as effectors, *ZjPCAP-LUC* and *ZjSGR-LUC* expressed earlier and reached their peak levels than was the GFP alone as control

effector (Figure 10C and 10D), implying that *ZjNAP* and *ZjNAC1* function as a potential positive senescence regulator. After being transfected as effectors, both *ZjAZF2*, *ZjNAC083*, *ZjARF1*, and *ZjPIL5* suppressed the expression of *ZjPCAP-LUC* and *ZjSGR-LUC* remarkably, implying their roles as potential negative senescence regulators. Interestingly, *ZjWRKY75* led to earlier induction in *ZjPCAP-LUC* and reduction in *ZjSGR-LUC* earlier than did the control. *ZjWRKY75* might play a dual role along senescence period, with a positive role in early stage and negative and attenuating role in late stage. However, the expression of two reporter genes when *ZjHB2* were expressed was comparable to that when the GFP control was expressed, indicating that *ZjHB2* is not likely to be senescence regulator, which is inconsistent with the function of Arabidopsis *HB-2* (ref). Overall, these 7 TFs DEGs are transcriptionally responsive to a broad range of senescence-inducing conditions and could be involved in senescence regulation in *Z. japonica*.

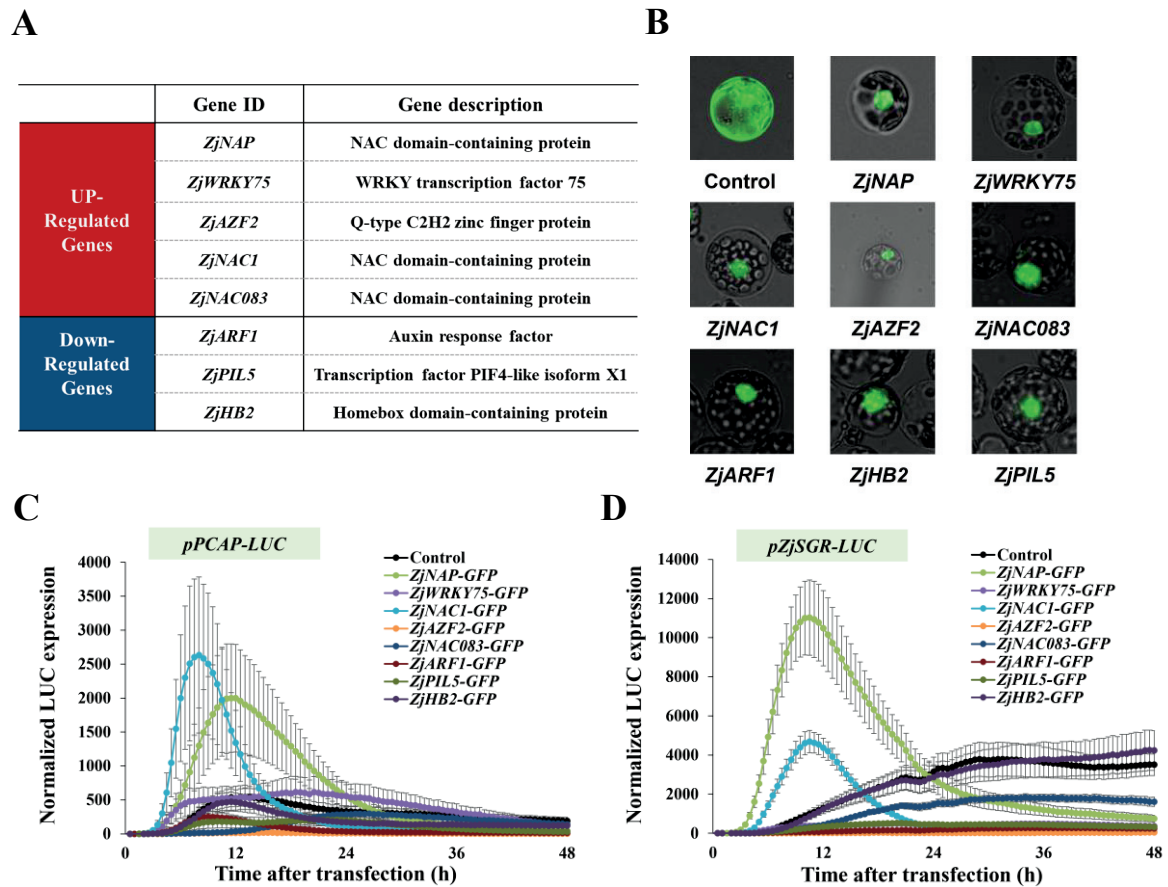


**Figure 10. Functional analysis of putative TF candidate genes through effector and reporter assay in Arabidopsis protoplasts.** (A) Information of putative TF candidate genes. (B) Expression and nuclear localization of proteins encoded by candidate genes in Arabidopsis protoplasts. Genes fused with GFP or GFP control were transiently expressed in Arabidopsis protoplasts. GFP signals were captured with a fluorescence microscope after 24 h of transfection. (C-D) Expression of *ZjPCAP-LUC* (C) and *ZjSGR-LUC* (D) reporters were examined when the indicated effector was co-expressed. 35S:RLUC was used as a normalization factor.

## **Functional assessment of TF candidate genes for the regulation of senescence responses in heterologous tobacco leaves**

Transient expression-based protoplast assay has been widely used for assessing regulatory roles of genes interested, based on their effect on promoter-driven reporter and can also be used as senescence assay (Yoo et al., 2007; Doan et al., 2022). However, the promoter activity can be changed by indirect or artificial perturbation effect of genes overexpressed in cells (Faraco et al., 2011). As an alternative approach for functional investigation in the senescence regulation, senescence responses in tobacco transiently overexpressing TF DEGs were examined under the dark. *ZjNAP* and *ZjNAC1* was selected as test sets for this senescence assay. Leaves expressing GFP control exhibited no detectable changes at DAT7 in the dark, whereas leaves expressing *ZjNAP* or *ZjNAC1* turned into yellow at DAT7 (Figure 11A). Furthermore, *ZjNAP*- and *ZjNAC1*- expressing leaves produced significantly lower levels in Fv/Fm value and in chlorophyll contents than GFP-expressing control leaves (Figure 11B and 11C). These results indicate that *ZjNAP* and *ZjNAC1* overexpression cause early leaf senescence in tobacco, which are consistent with the results shown in protoplast assay. These further supported validity of our results obtained through protoplast-based senescence assay and 7 TFs DEGs could have a potential to affect senescence traits in *Z. japonica* when they are perturbed.

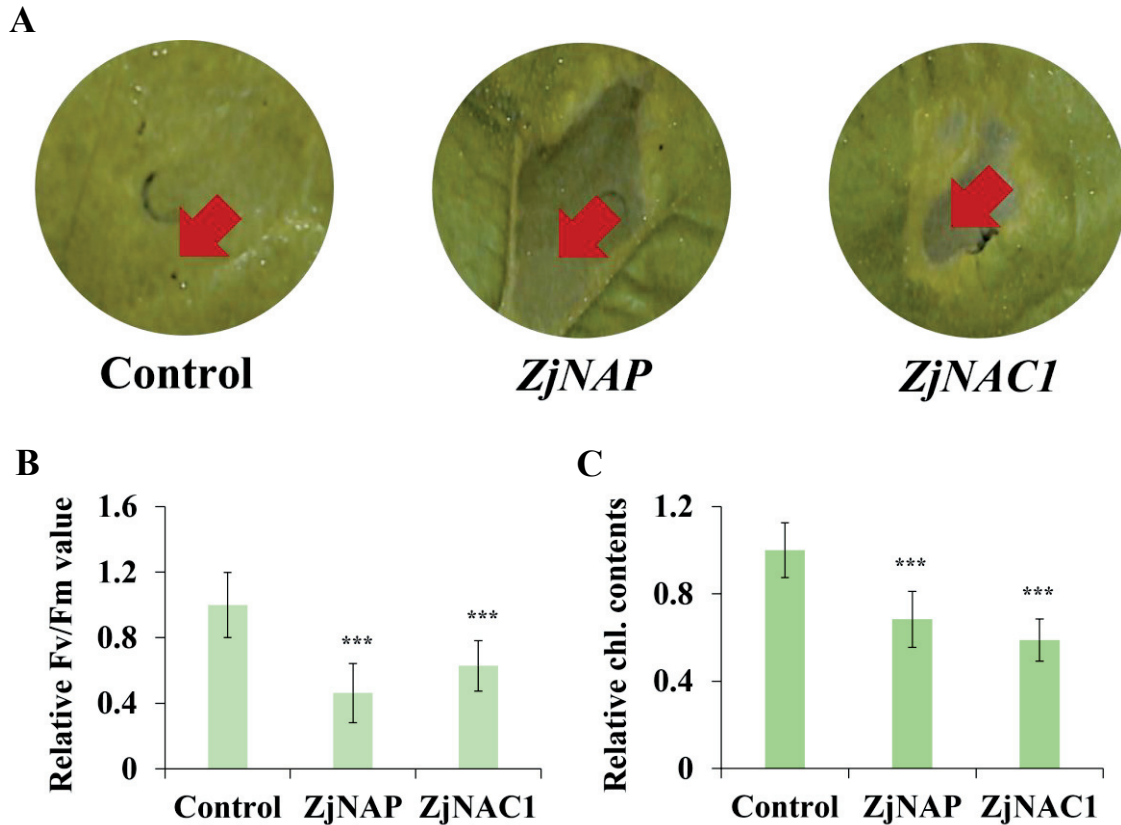


**Figure 11. Dark-induced senescence responses when TF candidate genes were over-expressed in tobacco using an *Agrobacterium*-mediated transient expression.** (A) Representative *N. benthamiana* leaves expressing eGFP, *ZjNAP*, or *ZjNAC1* under a 7-day dark treatment. The position used for assay in (B) and (C) is marked by red arrows. (B-C) Fv/Fm value (B) and relative chlorophyll contents (C) at 7 days after dark treatment. Data represent mean  $\pm$  SE. The asterisk indicates a significant difference (\*\*\*)  $P < 0.001$ , based on student's t-test.

## DISCUSSION

*Z. japonica* is a popular warm-season turfgrass with high economic value and widely used as decorative covers in many places including garden, park, sport field, and golf courses. However, one of limitations in *Z. japonica* is early yellowing in fall (Zhang et al., 2022). Short green period of *Z. japonica* can be adjusted by senescence control (Guan et al., 2022). Therefore, delaying leaf senescence in *Z. japonica* is an effective means to extend the green phase and increase its economic value.

Leaf senescence is the ultimate stage of leaf development and is a complex process. Although leaf senescence is common and acquired developmental events, senescence responses differ among species (Panchen et al., 2015; Kim et al., 2016b; Chai et al., 2019). Senescence is considered as one of important economic traits in many crops, but molecular events underlying senescence in *Z. Japonica* are largely unknown. The onset of senescence is regulated mainly by leaf age, but also affected by external stress (e.g. salt treatment) and limited energy levels (e.g. dark treatment). In this study, comparative transcriptomic analysis in age-, dark-, and salt-induced senescence were conducted for comprehensive understanding of the molecular mechanisms underlying *Z. japonica* leaf senescence and further identification of senescence regulatory genes that can be used for genetic modification to delay leaf senescence in *Z. japonica*.

Chlorophyll breakdown is a typical physiological marker for a wide range of leaf senescence responses triggered by age, stress, hormone, and dark (Song et al., 2014). By observing the leaf yellowing as well as chlorophyll content measurements in leaves, the senescence progression can be monitored and compared in different

senescence-inducing conditions. Since molecular responses in early senescence are divergent among different senescence conditions, comparative transcriptome responses should be conducted in similar and early stage of senescence (Zhao et al., 2020). It is also regarded that early senescence stage is useful to identify regulatory genes for genetic resource in regulating leaf senescence (Lim et al., 2007b). In this study, 20% chlorophyll loss in senescing leaves was used as early senescence stages (Figure 1A and 1D) as indicated in other studies (Woo et al., 2010; Kim et al., 2018a). Functional classification of transcriptomic responses during age-, dark- and salt-induced senescence conditions explain the biological processes that occurs in *Z. japonica* leaf senescence (Figure 3). These different senescence conditions shared the processes of amino acid degradation and photosynthesis as up and down-regulated biological processes, respectively. Among up-regulated processes, program cell death, cell wall reorganization, and solute transport are representative biological processes that are enriched in age-, dark-, and salt-induced senescence, respectively. Cytoskeleton reorganization, glycolysis, and TCP transcription factor are down-regulated processes in in age-, dark-, and salt-induced senescence, respectively. These results are consistent with previous findings in transcriptome analysis in *Arabidopsis* leaf senescence (Woo et al., 2016; Breeze et al, 2012; Kim et al., 2018; Allu et al., 2014). Interestingly, chromatin organization and gibberellin action are also enriched in up- and down-regulated processes in age-induced leaf senescence, respectively, which have not been reported yet, in my knowledge. These might be specifically related to *Z. japonica* leaf senescence.



Our transcriptome analysis also identified lots of sDEGs and cDEGs in senescence-induced conditions (Figure 4) and some of them were also validated as DEGs in independent samples (Figures 6 and 8). Six sDEGs and thirteen cDEGs validated can be used as markers for dissecting senescence triggering factors and exploring senescence responses, respectively.

Transcription factors (TF) have been shown to be crucial components as hubs in the senescence regulatory network by regulating transcription of downstream genes (Balazadeh et al., 2008). 55 up-regulated TFs and 8 down-regulated TF cDEGs was identified and most of these TFs belong to the NAC, WRKY, bHLH, and ARF families (Figure 7). NAC transcription factors have been shown to have an important part in chlorophyll breakdown and leaf senescence, as well as being actively implicated in ABA, MeJA, and ethylene signalling, which can counteract leaf senescence (Balazadeh et al., 2008; Takasaki et al., 2015). The ARF TF family plays a major part in abiotic and biotic stress defense responses, while the bHLH, MYB, and WRKY families are the main families that have been implicated in mediating senescence (Tolosa and Zhang, 2020; Dong et al., 2022). It is no doubt that TF DEGs identified in this study also plays an important role in senescence regulation by mediating many senescence-related biological processes.

Although many transcriptomic studies regarding on senescence in various non-model plants have identified many transcription factors that may be associated with leaf senescence, their functional role remains unsolved (Woo et al., 2013; Fraga et al., 2021; Zhang et al., 2021b). Functional studies using their knock-out or transgenic approaches are time- and resource-consuming works (Mahmood et al., 2022). For a

rapid functional evaluation for candidate genes in senescence regulation, transient expression system using *Arabidopsis* protoplasts was used. The protoplast transient expression system provides a platform for rapid and high-throughput assay along with relevant promoters-driven LUC reporters (Huo et al., 2017). *ZjSGR* and *ZjPCAP* promoters were selected as reporter genes, based on different kinetic but strong induction patterns during senescence (Figure 10C and 10D). Five up-regulated and three down-regulated TF DEGs, members of the ARF, NAC, C2H2, and WRKY families, was selected for functional assay in the protoplast, based on their kinetic expression patterns (Figure 9). Protoplast-based senescence assay revealed that *ZjNAP* and *ZjNAC1* function as positive senescence regulators, while *ZjNAC083*, *ZjAZF2*, *ZjARF1*, and *ZjPIL5* do as negative senescence regulators (Figure 10). Functional activity of *ZjNAP* and *ZjNAC1* was further confirmed by physiological senescence responses in tobacco leaves (Figure 11). Interestingly, *ZjAZF2* and *ZjNAC083* were identified as up-regulated DEGs, but function as negative senescence regulators, implying that these act as a molecular brake to slow down the senescence process or as a molecular breaker to shutdown inappropriate onset of senescence along aging, like NAC troika (Kim et al., 2018a). Functional assessment based on rapid senescence assay using protoplast and tobacco transient expression system support a possibility that seven TFs likely function as senescence regulatory genes in *Z. japonica*. In future studies, gene editing and overexpression approaches will be applied for these putative positive and negative senescence regulators to delay leaf senescence, respectively, which will be able to generate the needed evergreen trait in *Z. japonica*.

In summary, the comparative transcriptome analysis in age-, dark-, and salt-induced senescence allows us to obtain a comprehensive molecular understanding of transcription events during *Z. japonica* leaf senescence and further provides a potential genetic resource for the future breeding of *Z. japonica* with a long green phase.

## CONCLUSION

In this study, I performed comparative transcriptome analysis to understand senescence responses triggered by age, dark, and salt through a high-throughput RNA sequencing in *Z. japonica*. The differentially expressed genes (DEGs) which responded to dark, salt, or age-induced senescence accounted for 23.46, 17.60, and 3.88% among expressed genes, respectively, and the DEGs which commonly responded to all three conditions (cDEGs) accounted for 2.13%. Gene set enrichment analysis for functional characterization of the transcriptome during senescence revealed many convergent and distinct biological processes were required for each senescence response; for example, “degradation of fatty acid and amino acid” were commonly affected in all senescence conditions, while “programmed cell death (PCD) system”, “biosynthesis and degradation processes of hemicellulose” and “primary active transport of solute” were specifically enriched of age-, dark-, and salt-induced senescence, respectively. I also found that NAC, WRKY, bHLH, and ARF were major DEG TFs groups that are involved in the transcriptional regulation of DEGs during leaf senescence. Transient expression of ZjNAP, ZjWRKY75, ZjARF2, ZjNAC1, ZjNAC083, ZjARF1, and ZjPIL5 as effectors in protoplasts altered the expression of senescence promoter-driven LUC reporters, indicating that these TF cDEGs likely to function as senescence regulators. Additionally, functional activity of ZjNAC and ZjNAP in senescence regulation were validated in dark-induced senescence assay in tobacco leaves through their transient expression. Overall, this study will provide new insights into molecular mechanisms of *Z. japonica* leaf senescence and potential gene

resources to improve the economic value of *Z. japonica* by extending the leaf greening period.

## REFERENCES

- Akhtar, S., Ahmad, A., Jha, S.R., and Ahmad, J.** (2019). Regulation of Leaf Senescence by Macromolecule Degradation and Hormones. In *Senescence Signalling and Control in Plants*, pp. 61-97.
- Allu, A.D., Soja, A.M., Wu, A., Szymanski, J., and Balazadeh, S.** (2014). Salt stress and senescence: identification of cross-talk regulatory components. *J Exp Bot* **65**, 3993-4008.
- Balazadeh, S., Riano-Pachon, D.M., and Mueller-Roeber, B.** (2008). Transcription factors regulating leaf senescence in *Arabidopsis thaliana*. *Plant Biol (Stuttg)* **10 Suppl 1**, 63-75.
- Bengoa Luoni, S., Astigueta, F.H., Nicosia, S., Moschen, S., Fernandez, P., and Heinz, R.** (2019). Transcription Factors Associated with Leaf Senescence in Crops. *Plants (Basel)* **8**.
- Besseau, S., Li, J., and Palva, E.T.** (2012). WRKY54 and WRKY70 cooperate as negative regulators of leaf senescence in *Arabidopsis thaliana*. *Journal of Experimental Botany* **63**, 2667-2679.
- Bolger, A.M., Lohse, M., and Usadel, B.** (2014). Trimmomatic: a flexible trimmer for Illumina sequence data. *Bioinformatics* **30**, 2114-2120.
- Breeze, E., Harrison, E., McHattie, S., Hughes, L., Hickman, R., Hill, C., Kiddle, S., Kim, Y.S., Penfold, C.A., Jenkins, D., Zhang, C., Morris, K., Jenner, C., Jackson, S., Thomas, B., Tabrett, A., Legaie, R., Moore, J.D., Wild, D.L., Ott, S., Rand, D., Beynon, J., Denby, K., Mead, A., and Buchanan-Wollaston, V.** (2011). High-resolution temporal profiling of transcripts during *Arabidopsis* leaf senescence reveals a distinct chronology of processes and regulation. *Plant Cell* **23**, 873-894.
- Buchanan-Wollaston, V., Page, T., Harrison, E., Breeze, E., Lim, P.O., Nam, H.G., Lin, J.F., Wu, S.H., Swidzinski, J., Ishizaki, K., and Leaver, C.J.** (2005). Comparative transcriptome analysis reveals significant differences in gene expression and signalling pathways between developmental and dark/starvation-induced senescence in *Arabidopsis*. *Plant Journal* **42**, 567-585.
- Chai, M., Guo, Z.Y., Shi, X., Li, Y.B., Tang, J.H., and Zhang, Z.H.** (2019). Dissecting the Regulatory Network of Leaf Premature Senescence in Maize (*Zea mays* L.) Using Transcriptome Analysis of ZmELS5 Mutant. *Genes-Basel* **10**.
- Cheng, X.X., Dai, X.M., Zeng, H.M., Li, Y.X., Tang, W., and Han, L.B.** (2009). Gene expression involved in dark-induced leaf senescence in zoysiagrass (*Zoysia japonica*). *Plant Biotechnology Reports* **3**, 285-292.
- Doan, P.P.T., Kim, J.H., and Kim, J.** (2022). Rapid Investigation of Functional Roles of Genes in Regulation of Leaf Senescence Using *Arabidopsis* Protoplasts. *Front Plant Sci* **13**, 818239.

**Dong, S., Sang, L., Xie, H., Chai, M., and Wang, Z.Y.** (2021). Comparative Transcriptome Analysis of Salt Stress-Induced Leaf Senescence in *Medicago truncatula*. *Front Plant Sci* **12**, 666660.

**Dong, S., Pang, W., Liu, Z., Li, H., Zhang, K., Cong, L., Yang, G., Wang, Z.Y., and Xie, H.** (2022). Transcriptome Analysis of Leaf Senescence Regulation Under Alkaline Stress in *Medicago truncatula*. *Front Plant Sci* **13**, 881456.

**Faraco, M., Di Sansebastiano, G.P., Spelt, K., Koes, R.E., and Quattrocchio, F.M.** (2011). One protoplast is not the other! *Plant physiology* **156**, 474-478.

**Fraga, O.T., de Melo, B.P., Quadros, I.P.S., Reis, P.A.B., and Fontes, E.P.B.** (2021). Senescence-Associated Glycine max (Gm)NAC Genes: Integration of Natural and Stress-Induced Leaf Senescence. *International Journal of Molecular Sciences* **22**.

**Guan, J., Teng, K., Yue, Y., Guo, Y., Liu, L., Yin, S., and Han, L.** (2022). *Zoysia japonica* Chlorophyll b Reductase Gene NOL Participates in Chlorophyll Degradation and Photosynthesis. *Front Plant Sci* **13**, 906018.

**Guo, Y., and Gan, S.S.** (2014). Translational researches on leaf senescence for enhancing plant productivity and quality. *J Exp Bot* **65**, 3901-3913.

**Guo, Y., Ren, G., Zhang, K., Li, Z., Miao, Y., and Guo, H.** (2021). Leaf senescence: progression, regulation, and application. *Molecular Horticulture* **1**.

**Hayakawa, T., Toda, T., Ping, Q., Mghalu, J.M., Yaguchi, S., and Hyakumachi, M.** (2006). A New Subgroup of *Rhizoctonia* AG-D, AG-D III, Obtained from Japanese *Zoysia* Grass Exhibiting Symptoms of a New Disease. *Plant Dis* **90**, 1389-1394.

**Huo, A., Chen, Z., Wang, P., Yang, L., Wang, G., Wang, D., Liao, S., Cheng, T., Chen, J., and Shi, J.** (2017). Establishment of transient gene expression systems in protoplasts from *Liriodendron* hybrid mesophyll cells. *PLoS One* **12**, e0172475.

**Jan, A., Maruyama, K., Todaka, D., Kidokoro, S., Abo, M., Yoshimura, E., Shinozaki, K., Nakashima, K., and Yamaguchi-Shinozaki, K.** (2013). OsTZF1, a CCCH-Tandem Zinc Finger Protein, Confers Delayed Senescence and Stress Tolerance in Rice by Regulating Stress-Related Genes. *Plant Physiology* **161**, 1202-1216.

**Jehanzeb, M., Zheng, X., and Miao, Y.** (2017). The Role of the S40 Gene Family in Leaf Senescence. *Int J Mol Sci* **18**.

**Kidokoro, S., Watanabe, K., Otori, T., Moriwaki, T., Maruyama, K., Mizoi, J., Htwe, N.M.P.S., Fujita, Y., Sekita, S., Shinozaki, K., and Yamaguchi-Shinozaki, K.** (2015). Soybean DREB1/CBF-type transcription factors function in heat and drought as well as cold stress-responsive gene expression. *Plant Journal* **81**, 505-518.

**Kim, D., Paggi, J.M., Park, C., Bennett, C., and Salzberg, S.L.** (2019). Graph-based genome alignment and genotyping with HISAT2 and HISAT-genotype. *Nat Biotechnol* **37**, 907-915.

**Kim, H.J., Nam, H.G., and Lim, P.O.** (2016a). Regulatory network of NAC transcription factors in leaf senescence. *Curr Opin Plant Biol* **33**, 48-56.

**Kim, H.J., Park, J.H., Kim, J., Kim, J.J., Hong, S., Kim, J., Kim, J.H., Woo, H.R., Hyeon, C., Lim, P.O., Nam, H.G., and Hwang, D.** (2018a). Time-evolving genetic networks reveal a NAC troika that negatively regulates leaf senescence in Arabidopsis. *P Natl Acad Sci USA* **115**, E4930-E4939.

**Kim, H.J., Hong, S.H., Kim, Y.W., Lee, I.H., Jun, J.H., Phee, B.K., Rupak, T., Jeong, H., Lee, Y., Hong, B.S., Nam, H.G., Woo, H.R., and Lim, P.O.** (2014). Gene regulatory cascade of senescence-associated NAC transcription factors activated by ETHYLENE-INSENSITIVE2-mediated leaf senescence signalling in Arabidopsis. *J Exp Bot* **65**, 4023-4036.

**Kim, J., and Somers, D.E.** (2010). Rapid assessment of gene function in the circadian clock using artificial microRNA in Arabidopsis mesophyll protoplasts. *Plant Physiol* **154**, 611-621.

**Kim, J., Woo, H.R., and Nam, H.G.** (2016b). Toward Systems Understanding of Leaf Senescence: An Integrated Multi-Omics Perspective on Leaf Senescence Research. *Mol Plant* **9**, 813-825.

**Kim, J., Kim, J.H., Lyu, J.I., Woo, H.R., and Lim, P.O.** (2018b). New insights into the regulation of leaf senescence in Arabidopsis. *Journal of Experimental Botany* **69**, 787-799.

**Kong, X., Luo, Z., Dong, H., Eneji, A.E., Li, W., and Lu, H.** (2013). Gene expression profiles deciphering leaf senescence variation between early- and late-senescence cotton lines. *PLoS One* **8**, e69847.

**Lee, R.H., Wang, C.H., Huang, L.T., and Chen, S.C.** (2001). Leaf senescence in rice plants: cloning and characterization of senescence up-regulated genes. *J Exp Bot* **52**, 1117-1121.

**Lee, S., and Masclaux-Daubresse, C.** (2021). Current Understanding of Leaf Senescence in Rice. *International Journal of Molecular Sciences* **22**.

**Li, J., Yang, Y., Iqbal, A., Qadri, R., Shi, P., Wang, Y., Wu, Y., Fan, H., and Wu, G.** (2019). Correlation analysis of cold-related gene expression with physiological and biochemical indicators under cold stress in oil palm. *PLoS One* **14**, e0225768.

**Lim, C., Chung, B.Y., Pitman, J.L., McGill, J.J., Pradhan, S., Lee, J., Keegan, K.P., Choe, J., and Allada, R.** (2007a). Clockwork orange encodes a transcriptional repressor important for circadian-clock amplitude in *Drosophila*. *Curr Biol* **17**, 1082-1089.



- Lim, P.O., Kim, H.J., and Nam, H.G.** (2007b). Leaf senescence. *Annu Rev Plant Biol* **58**, 115-136.
- Lin, T., Zhou, R., Bi, B., Song, L., Chai, M., Wang, Q., and Song, G.** (2020). Analysis of a radiation-induced dwarf mutant of a warm-season turf grass reveals potential mechanisms involved in the dwarfing mutant. *Sci Rep* **10**, 18913.
- Livak, K.J., and Schmittgen, T.D.** (2001). Analysis of relative gene expression data using real-time quantitative PCR and the 2(T)(-Delta Delta C) method. *Methods* **25**, 402-408.
- Loch, D.S., Aldous, D.E., McMaugh, P.E., Colmer, T.D., Martin, P.M., Ford, P.G., Neylan, J.J., Burrup, D.H., and Dempsey, F.L.** (2016). Turfgrass education, research and information in Australia: history, development and implications. *Acta Hort* **1122**, 9-17.
- Love, M.I., Huber, W., and Anders, S.** (2014). Moderated estimation of fold change and dispersion for RNA-seq data with DESeq2. *Genome Biol* **15**, 550.
- Mahmood, K., Torres-Jerez, I., Krom, N., Liu, W., and Udvardi, M.K.** (2022). Transcriptional Programs and Regulators Underlying Age-Dependent and Dark-Induced Senescence in *Medicago truncatula*. *Cells* **11**.
- Miao, Y., Laun, T., Zimmermann, P., and Zentgraf, U.** (2004). Targets of the WRKY53 transcription factor and its role during leaf senescence in *Arabidopsis*. *Plant Mol Biol* **55**, 853-867.
- Panchen, Z.A., Primack, R.B., Gallinat, A.S., Nordt, B., Stevens, A.D., Du, Y.J., and Fahey, R.** (2015). Substantial variation in leaf senescence times among 1360 temperate woody plant species: implications for phenology and ecosystem processes. *Ann Bot-London* **116**, 865-873.
- Park, J.K., Liu, X., Strauss, T.J., McKearin, D.M., and Liu, Q.** (2007). The miRNA pathway intrinsically controls self-renewal of *Drosophila* germline stem cells. *Curr Biol* **17**, 533-538.
- Pertea, M., Pertea, G.M., Antonescu, C.M., Chang, T.C., Mendell, J.T., and Salzberg, S.L.** (2015). StringTie enables improved reconstruction of a transcriptome from RNA-seq reads. *Nat Biotechnol* **33**, 290-295.
- Podzimska-Sroka, D., O'Shea, C., Gregersen, P.L., and Skriver, K.** (2015). NAC Transcription Factors in Senescence: From Molecular Structure to Function in Crops. *Plants (Basel)* **4**, 412-448.
- Qi, T.C., Wang, J.J., Huang, H., Liu, B., Gao, H., Liu, Y.L., Song, S.S., and Xie, D.X.** (2015). Regulation of Jasmonate-Induced Leaf Senescence by Antagonism between bHLH Subgroup IIIe and IIIId Factors in *Arabidopsis*. *Plant Cell* **27**, 1634-1649.
- Robatzek, S., and Somssich, I.E.** (2001). A new member of the *Arabidopsis* WRKY transcription factor family, AtWRKY6, is associated with both senescence- and defence-related processes. *Plant Journal* **28**, 123-133.

**Sekhon, R.S., Childs, K.L., Santoro, N., Foster, C.E., Buell, C.R., de Leon, N., and Kaeppler, S.M.** (2012). Transcriptional and Metabolic Analysis of Senescence Induced by Preventing Pollination in Maize. *Plant Physiology* **159**, 1730-1744.

**Soledad, T.R., Monica, C., Giorgio, M., Ida, R., and Francisco, B.J.** (2021). *ATHB2* is a negative regulator of germination in *Arabidopsis thaliana* seeds. *Sci Rep-Uk* **11**.

**Song, Y., Yang, C., Gao, S., Zhang, W., Li, L., and Kuai, B.** (2014). Age-triggered and dark-induced leaf senescence require the bHLH transcription factors PIF3, 4, and 5. *Mol Plant* **7**, 1776-1787.

**Takasaki, H., Maruyama, K., Takahashi, F., Fujita, M., Yoshida, T., Nakashima, K., Myouga, F., Toyooka, K., Yamaguchi-Shinozaki, K., and Shinozaki, K.** (2015). SNAC-As, stress-responsive NAC transcription factors, mediate ABA-inducible leaf senescence. *Plant J* **84**, 1114-1123.

**Tanaka, H., Hirakawa, H., Kosugi, S., Nakayama, S., Ono, A., Watanabe, A., Hashiguchi, M., Gondo, T., Ishigaki, G., Muguerza, M., Shimizu, K., Sawamura, N., Inoue, T., Shigeki, Y., Ohno, N., Tabata, S., Akashi, R., and Sato, S.** (2016). Sequencing and comparative analyses of the genomes of zoysiagrasses. *DNA Res* **23**, 171-180.

**Teng, K., Chang, Z.H., Xiao, G.Z., Guo, W.E., Xu, L.X., Chao, Y.H., and Han, L.B.** (2016a). Molecular cloning and characterization of a chlorophyll degradation regulatory gene (*ZjSGR*) from *Zoysia japonica*. *Genet Mol Res* **15**.

**Teng, K., Chang, Z., Li, X., Sun, X., Liang, X., Xu, L., Chao, Y., and Han, L.** (2016b). Functional and RNA-Sequencing Analysis Revealed Expression of a Novel Stay-Green Gene from *Zoysia japonica* (*ZjSGR*) Caused Chlorophyll Degradation and Accelerated Senescence in *Arabidopsis*. *Front Plant Sci* **7**, 1894.

**Teng, K., Yue, Y., Zhang, H., Li, H., Xu, L., Han, C., Fan, X., and Wu, J.** (2021). Functional Characterization of the Pheophytinase Gene, *ZjPPH*, From *Zoysia japonica* in Regulating Chlorophyll Degradation and Photosynthesis. *Front Plant Sci* **12**, 786570.

**Thimm, O., Blasing, O., Gibon, Y., Nagel, A., Meyer, S., Kruger, P., Selbig, J., Muller, L.A., Rhee, S.Y., and Stitt, M.** (2004). MAPMAN: a user-driven tool to display genomics data sets onto diagrams of metabolic pathways and other biological processes. *Plant J* **37**, 914-939.

**Tolosa, L.N., and Zhang, Z.** (2020). The Role of Major Transcription Factors in Solanaceous Food Crops under Different Stress Conditions: Current and Future Perspectives. *Plants (Basel)* **9**.

**Uauy, C., Distelfeld, A., Fahima, T., Blechl, A., and Dubcovsky, J.** (2006). A NAC Gene regulating senescence improves grain protein, zinc, and iron content in wheat. *Science* **314**, 1298-1301.

**Usadel, B., Poree, F., Nagel, A., Lohse, M., Czedik-Eysenberg, A., and Stitt, M.** (2009). A guide to using MapMan to visualize and compare Omics data in plants: a case study in the crop species, Maize. *Plant Cell Environ* **32**, 1211-1229.

**Uzelac, B., Janosevic, D., Simonovic, A., Motyka, V., Dobrev, P.I., and Budimir, S.** (2016). Characterization of natural leaf senescence in tobacco (*Nicotiana tabacum*) plants grown in vitro. *Protoplasma* **253**, 259-275.

**Wang, H.L., Zhang, Y., Wang, T., Yang, Q., Yang, Y.L., Li, Z., Li, B.S., Wen, X., Li, W.Y., Yin, W.L., Xia, X.L., Guo, H.W., and Li, Z.H.** (2021). An alternative splicing variant of PtRD26 delays leaf senescence by regulating multiple NAC transcription factors in *Populus*. *Plant Cell* **33**, 1594-1614.

**Wei, S., Du, Z., Gao, F., Ke, X., Li, J., Liu, J., and Zhou, Y.** (2015). Global Transcriptome Profiles of 'Meyer' Zoysiagrass in Response to Cold Stress. *PLoS One* **10**, e0131153.

**Woo, H.R., Kim, H.J., Nam, H.G., and Lim, P.O.** (2013). Plant leaf senescence and death - regulation by multiple layers of control and implications for aging in general. *J Cell Sci* **126**, 4823-4833.

**Woo, H.R., Kim, J.H., Kim, J., Kim, J., Lee, U., Song, I.J., Kim, J.H., Lee, H.Y., Nam, H.G., and Lim, P.O.** (2010). The RAV1 transcription factor positively regulates leaf senescence in *Arabidopsis*. *J Exp Bot* **61**, 3947-3957.

**Yoo, S.D., Cho, Y.H., and Sheen, J.** (2007). *Arabidopsis* mesophyll protoplasts: a versatile cell system for transient gene expression analysis. *Nat Protoc* **2**, 1565-1572.

**Zentgraf, U., Laun, T., and Miao, Y.** (2010). The complex regulation of WRKY53 during leaf senescence of *Arabidopsis thaliana*. *Eur J Cell Biol* **89**, 133-137.

**Zhang, H., and Zhou, C.** (2013). Signal transduction in leaf senescence. *Plant Mol Biol* **82**, 539-545.

**Zhang, H.Y., Zhang, L.P., Wu, S.G., Chen, Y.L., Yu, D.Q., and Chen, L.G.** (2021a). AtWRKY75 positively regulates age-triggered leaf senescence through gibberellin pathway. *Plant Diversity* **43**, 331-340.

**Zhang, J., Zhang, Z., Liu, W., Li, L., Han, L., Xu, L., and Zhao, Y.** (2022). Transcriptome Analysis Revealed a Positive Role of Ethephon on Chlorophyll Metabolism of *Zoysia japonica* under Cold Stress. *Plants (Basel)* **11**.

**Zhang, W.Y., Xu, Y.C., Li, W.L., Yang, L., Yue, X., Zhang, X.S., and Zhao, X.Y.** (2014). Transcriptional analyses of natural leaf senescence in maize. *PLoS One* **9**, e115617.

**Zhang, Y.M., Guo, P.R., Xia, X.L., Guo, H.W., and Li, Z.H.** (2021b). Multiple Layers of Regulation on Leaf Senescence: New Advances and Perspectives. *Frontiers in Plant Science* **12**.

**Zhao, Z., Zhang, J.W., Lu, S.H., Zhang, H., Liu, F., Fu, B., Zhao, M.Q., and Liu, H. (2020).** Transcriptome divergence between developmental senescence and premature senescence in *Nicotiana tabacum* L. *Sci Rep-Uk* **10**.

**Zhou, X., Jiang, Y., and Yu, D. (2011).** WRKY22 transcription factor mediates dark-induced leaf senescence in *Arabidopsis*. *Mol Cells* **31**, 303-313.

## ACKNOWLEDGMENT

I would like to express my deepest gratitude to all those who have helped and supported me so much in the process of writing my thesis.

Firstly, my warmest thanks to my supervisor, Prof. Jeongsik Kim, who provided me with many helpful comments and suggestions with great patient and gave me profound encouragement during my graduate studies. In addition, I am honored to have benefited from his personality and academic attitude, which I will always appreciate. My gratitude to him is boundless.

My heartfelt thanks to Dr. Jin Hee Kim for editing my master manuscript and giving me a lot of help in my experiments and life, and for making me feel warm in this foreign country. I would also like to thank my lab members Doan Phan Phuong Thao and Nguyen Nguyen Chuong in the Plant Molecular Genomics Lab for their warmth and help during my master's degree.

I am also deeply grateful to my family, who has been an essential pillar in my life from afar. Not only that, but I am very grateful to my friends for their companionship and listening, whether it is quarrels, sadness or happiness, because they have brought lighter to my life at Jeju International University and kept me going to the end.

Finally, I hope that this thesis will not be the end of academic thinking and that the previous sentence is not just a hope.